

SANDIA REPORT

SAND86-1264 • UC-70

Unlimited Release

Printed August 1987

Nevada Nuclear Waste Storage Investigations Project

Specification of a Test Problem for HYDROCOIN Level 3 Case 2: Sensitivity Analysis for Deep Disposal in Partially Saturated, Fractured Tuff

Robert W. Prindle

Prepared by
Sandia National Laboratories
Albuquerque, New Mexico 87185 and Livermore, California 94550
for the United States Department of Energy
under Contract DE-AC04-76DP00789

HYDROLOGY DOCUMENT NUMBER 119



Issued by Sandia National Laboratories, operated for the United States Department of Energy by Sandia Corporation.

NOTICE: This report was prepared as an account of work sponsored by an agency of the United States Government. Neither the United States Government nor any agency thereof, nor any of their employees, nor any of their contractors, subcontractors, or their employees, makes any warranty, express or implied, or assumes any legal liability or responsibility for the accuracy, completeness, or usefulness of any information, apparatus, product, or process disclosed, or represents that its use would not infringe privately owned rights. Reference herein to any specific commercial product, process, or service by trade name, trademark, manufacturer, or otherwise, does not necessarily constitute or imply its endorsement, recommendation, or favoring by the United States Government, any agency thereof or any of their contractors or subcontractors. The views and opinions expressed herein do not necessarily state or reflect those of the United States Government, any agency thereof or any of their contractors or subcontractors.

Printed in the United States of America
Available from
National Technical Information Service
U.S. Department of Commerce
5285 Port Royal Road
Springfield, VA 22161

NTIS price codes
Printed copy: A03
Microfiche copy: A01

Nevada Nuclear Waste Storage Investigations Project

Specification of a Test Problem for HYDROCOIN Level 3 Case 2: Sensitivity Analysis for Deep Disposal in Partially Saturated, Fractured Tuff

Robert W. Prindle
Nevada Nuclear Waste Storage Investigations Project
Sandia National Laboratories
Albuquerque, NM 87185

Abstract

The international Hydrologic Code Intercomparison Project (HYDROCOIN) was formed to evaluate hydrogeologic models and computer codes and their use in performance assessment for high-level radioactive waste repositories. There are three principal activities in the HYDROCOIN Project: Level 1, verification and benchmarking of hydrologic codes; Level 2, validation of hydrologic models; and Level 3, sensitivity and uncertainty analyses of the models and codes. This report presents a test case defined for the HYDROCOIN Level 3 activity. The purposes of this test case are to explore the feasibility of applying various sensitivity-analysis methodologies to a highly nonlinear model of isothermal, partially saturated flow through fractured tuff, and to develop modeling approaches to implement the methodologies for sensitivity analysis. These analyses involve an idealized representation of a repository sited above the water table in a layered sequence of welded and nonwelded, fractured, volcanic tuffs. The analyses suggested here are divided into three groups with varying levels of complexity and computational difficulty: (1) one-dimensional, steady flow; (2) one-dimensional, nonsteady flow; and (3) two-dimensional, steady flow. Performance measures to be used to evaluate model sensitivities are also defined; the measures are related to regulatory criteria for containment of high-level radioactive waste.

Contents

List of Symbols	7
Introduction	9
Purpose	10
Overview of Proposed Analyses	10
Site Description	11
Conceptual Models	12
Mathematical Model for Partially Saturated Flow in a Compressible, Fractured Tuff	12
Saturation	13
Hydraulic Conductivity	13
Nonsteady-Flow Equation	13
Steady-Flow Equation	14
Flow Velocity of Water	14
Numerical-Convergence Criteria	14
Sensitivity Analyses for 1-D Flow	14
Description	14
Performance Measures	15
Steady Flow	15
Nonsteady Flow	15
Criterion for Nonnegligible Flow Volume	16
Base-Case Parameters	16
Variations	19
Sensitivity Analyses for 2-D Flow	19
Description	19
Simplified 2-D Analyses	20
Performance Measures	21
Base-Case Parameters	21
Variations	21
Mesh Design Considerations	22
References	23
APPENDIX A—Plots of Capacitance Coefficients and Hydraulic Conductivities	25
APPENDIX B—NNWSI Data Base Information	31

Figures

1 Generalized Hydrogeologic System	11
2 Stratigraphy for 1-D Base Cases (Cases 1 through 4)	15
3 Stratigraphy for 2-D Base Cases (Cases 5 and 6)	20
4a Stratigraphy for Simplified 2-D Analyses Using Units A, B, and C	20
4b Stratigraphy for Simplified 2-D Analyses Using Units C, D, and E	20

Tables

1 Hydrogeologic Units in the Unsaturated Zone	12
2 Coordinates of the Numbered Points for the 1-D Flow Analyses	15
3 Base-Case Values and Ranges of Properties for the Hydrologic Units in the Unsaturated Zone of the Tuff Site	17
4 Coordinates of the Numbered Points for the 2-D Flow Analyses	20

List of Symbols

K	hydraulic conductivity
\bar{K}	hydraulic conductivity tensor
n	porosity
\bar{q}	specific discharge
S	saturation
t	time
∇	velocity of water
z	elevation

Greek Symbols

α	curve-fitting parameter (primarily describes the pressure head at which desaturation begins)
α'_{bulk}	coefficient of consolidation
β	curve-fitting parameter (primarily describes the slope of the desaturation portion of the saturation curve)
β'_w	compressibility of water
∇	differential operator
λ	curve-fitting parameter = $\left(1 - \frac{1}{\beta}\right)$
σ'	stress in the rock mass
ρ	density of water
ψ	pressure head

Subscripts

f	fracture
m	matrix
f,b	bulk fracture values for a unit volume of fractured, porous media
r	residual
s	saturated

Nevada Nuclear Waste Storage Investigations Project

Specification of a Test Problem for HYDROCOIN Level 3 Case 2: Sensitivity Analysis for Deep Disposal in Partially Saturated, Fractured Tuff

Introduction

Mathematical models have been developed to describe the processes that are expected to occur in geologic repositories for high-level radioactive waste. These models are generally embodied in complex computer codes that will be used to assess the long-term safety of the proposed repositories. We need to demonstrate that the models are appropriate and adequate and that the codes that embody them are numerically correct. We also need to understand the limits of applicability and the sensitivities and uncertainties of the models and codes for the ranges of hydrologic and radionuclide-transport parameters that are expected to be encountered at the proposed repository sites.

Of the models that are used to assess the performance of a total repository system, those that describe the movement of groundwater at a potential repository site are especially important. The international Hydrologic Code Intercomparison Project (HYDROCOIN) was formed to evaluate hydrogeologic models and codes and their use in performance assessment for high-level-radioactive-waste repositories.

Hodgkinson et al., 1985, described the purposes of the HYDROCOIN project:

The primary aim of *Level 1* of HYDROCOIN is the *verification* of the numerical accuracy of groundwater flow codes by intercomparing their solutions to certain well-defined test problems and by comparison with analytical solutions.

Level 2 of HYDROCOIN is concerned with the *validation* of computer models in order to test their ability to describe the results of laboratory and field experiments.

HYDROCOIN Level 3 is concerned with the *application* of hydrogeological models in performance assessments, taking into account uncertainties in the models and data. In particular, *Level 3* is concerned with the sensitivity of results to characteristics of the site which are poorly known or which could change with time, and the associated uncertainties in the model predictions. Its aims are to explore alternative methodologies and calculational techniques for carrying out sensitivity and uncertainty analyses, to derive some general results which apply to each of a number of different geological settings, and to act as a forum for exchanges of ideas and information.

This paper presents a problem specification for a HYDROCOIN Level 3 sensitivity analysis of models that could be used to describe partially saturated flow through fractured tuff. The proposed analyses involve a nonlinear mathematical model and materials with highly nonlinear hydrologic properties. These analyses may be of interest to groups whose performance-assessment analyses involve any of the following: nonlinear analyses, partially saturated flow, combined matrix and fracture flow, volcanic tuffs, or layered materials with sharp layer boundaries and large contrasts in material properties.

The problem defined in this paper is entirely conceptual in character and is put forth strictly for the purposes of the HYDROCOIN Project. It is specifically not intended that the problem, as defined, be taken as representative of the potential tuff repository site being evaluated by the U.S. Department of Energy. The physical constants, analytical methods, and numerical results are therefore not to be construed as U.S. Department of Energy perceptions of the proposed tuff site.

Purpose

The purposes of the analyses outlined in this report are

- To explore the feasibility of applying various sensitivity-analysis methods to a highly nonlinear model of isothermal, partially saturated flow through layered, fractured tuff
- To develop approaches for site modeling that will help when implementing the methods for sensitivity analysis
- To investigate, for a particular mathematical model of partially saturated flow at an idealized site, the sensitivity of the output of the model to variations in its input

Sensitivity will be evaluated by observing the changes in performance measures that are based on model output. Because this mathematical model is intended for use in performance-assessment analyses, the performance measures chosen for these sensitivity analyses are directly related to the long-term performance of the site as a potential repository for high-level radioactive waste. Knowledge of the sensitivities of the performance measures to various inputs can then be used to decide where the greatest effort should be spent to refine conceptual models, to quantify parameters in the mathematical model, and to decide which parameters may be safely deleted when developing simplified models. Inputs that will be varied include both the values assigned to the parameters in the mathematical model and the conceptual models that describe the hydrogeology and geologic structure of the idealized site.

Overview of Proposed Analyses

Six sets of analyses are described in this report to provide a range of physical and analytical complexity that will allow interested HYDROCOIN Project teams to take on as much or as little work as desired. The sensitivity analyses proposed here are unquestionably difficult, and, depending on which cases are undertaken, personnel and computing costs could be high. Because of the level of technical difficulty and the potentially high costs, it may not be possible to complete all of these analyses within the framework of the HYDROCOIN project.

The six analysis sets are described in terms of base cases that include one-dimensional (1-D) and two-dimensional (2-D) conceptual flow models, steady and

nonsteady flow conditions, and both low and high initial fluxes to compare sensitivities during matrix-dominated and fracture-dominated flow. The base cases are

Case 1: 1-D, low flux, steady, matrix-dominated flow

Case 2: 1-D, high flux, steady, fracture-dominated flow

Case 3: 1-D, low flux, nonsteady, matrix-dominated flow

Case 4: 1-D, high flux, nonsteady, fracture-dominated flow

Case 5: 2-D, low flux, steady, matrix-dominated flow

Case 6: 2-D, high flux, steady, fracture-dominated flow

Cases 1 and 2 are the simplest but are sufficient to provide useful insights into the behavior of this unsaturated-flow system and into the process of modeling it. Because these cases involve 1-D, isothermal, steady-state flow, they can be analyzed using standard numerical solvers for ordinary differential equations. Such solvers are fast and efficient so a wide variety of methods for sensitivity analysis can readily be applied and compared. It should be noted that, in the analyses of 1-D, steady-state flow, the materials between the ground surface and the repository have no effect on flow conditions between the repository and the water table and can therefore be ignored.

Cases 3 through 6 are significantly more difficult than Cases 1 and 2, and they will require codes that use finite-element or finite-difference methods or some other technique such as dynamics of contours. These analyses can be expected to consume a large amount of computer time. Selected local sensitivity analyses should be within the reach of project teams using appropriate analytical tools. Global sensitivity analyses on Cases 3 through 6 are probably beyond the resources available within the HYDROCOIN Project.

We need to remember that the ultimate goal of this particular Level 3 exercise is to develop modeling approaches and sensitivity-analysis methods that will yield useful insights into the behavior of this complex hydrologic system. Even a simple comparison of changes in performance among the six base cases would be a valuable contribution. While it may not be possible to complete all of the suggested analyses during the HYDROCOIN Project, we still should be able to make significant progress toward this goal.

Site Description

The hydrogeologic system described here is shown schematically in Figure 1. The idealized site is made up of a sequence of ash-fall and ash-flow tuffs. The amount of welding, fracturing, and chemical alteration varies greatly from one layer to the next. Fracturing in all units is dominated by two sets of nearly vertical fractures and one set of horizontal fractures. Major fault zones cut through the entire vertical section.

The water table is relatively flat beneath most of the site. The repository horizon lies entirely within the partially saturated zone in Unit D. The principal hydrogeologic units that make up the unsaturated zone and will be considered in these analyses are briefly described in Table 1. Hydrologic characteristics vary greatly from one layer to another because of the differences in the degree of welding, fracturing, and chemical alteration.

Klavetter and Peters, 1986, have described three broad categories of hydrogeologic units in these tuffs:

1. Densely welded tuffs that are highly fractured. These units have low saturated matrix conductivities (10^{-11} m/s or less) and high saturated fracture conductivities. For a unit volume of rock, the total saturated conductivity of the fracture system is probably several orders of magnitude higher than the total saturated conductivity of the matrix. This group includes Units A, C, and D.
2. Nonwelded, vitric tuffs that have few fractures. These units have high saturated matrix conductivities (in the range of 10^{-6} to 10^{-8} m/s) and relatively low saturated fracture conductivities. This group includes Units B and Ev.
3. Nonwelded, zeolitized tuffs that have few fractures. These units have low saturated matrix conductivities (10^{-11} m/s or less) and low saturated fracture conductivities. The unit above the water table in this group is Unit Ez.

The contacts between these units generally tend to be sharp; thus, there can be extreme contrasts in hydraulic conductivities occurring over very short distances.

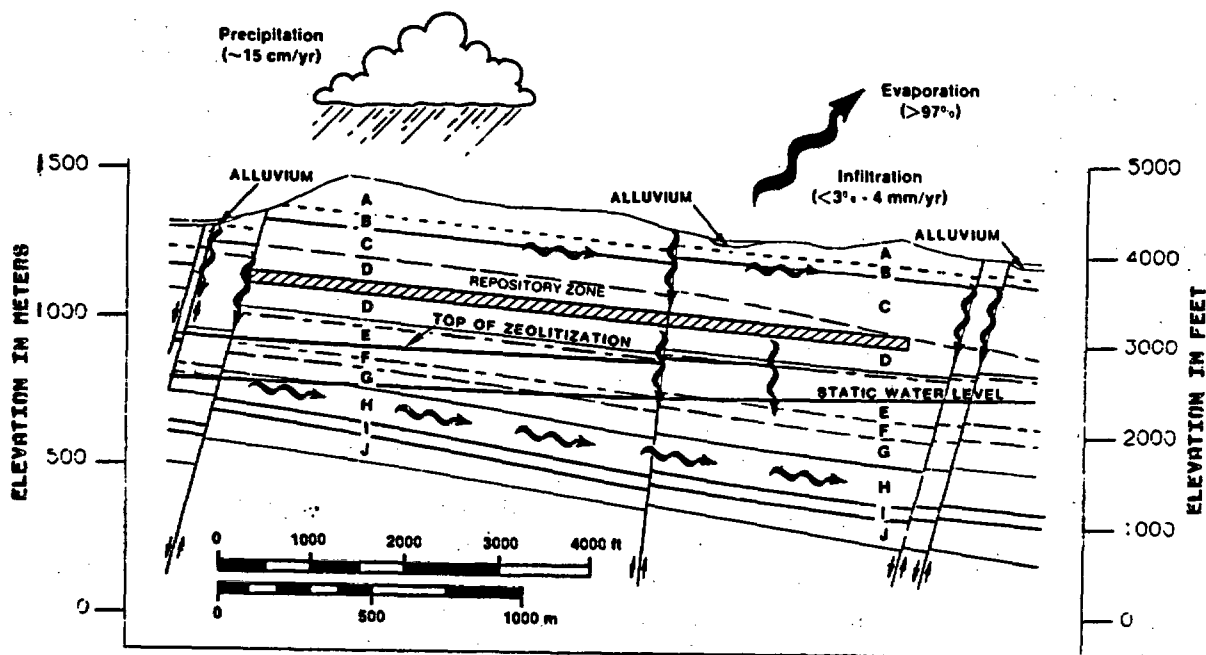


Figure 1. Generalized Hydrogeologic System

Table 1. Hydrogeologic Units in the Unsaturated Zone (after Ortiz et al., 1985)

Unit Name	Description
Unit A, welded	Moderately to densely welded, devitrified ash-flow tuff
Unit B, nonwelded	Partially welded to nowelded vitric tuffs
Unit C, welded, lithophysae-rich	Moderately to densely welded, devitrified ash-flow tuffs that locally contain more than approximately 10% by volume lithophysal cavities
Unit D, welded, lithophysae-poor	Moderately to densely welded, devitrified ash-flow tuffs that locally contain less than approximately 10% by volume lithophysal cavities
Unit E, nonwelded	Nonwelded ash-flows, bedded and reworked tuffs; includes both the vitric (Ev) and zeolitic (Ez) sections

Conceptual Models

Two conceptual models of flow that have been postulated for semi-arid and wetter climatic conditions have been characterized as:

1. One-dimensional, vertical, downward flow
2. Multidimensional flow, in particular with flow diverted laterally at layer contacts and from within the nonwelded units into the major structural features of the site

Both conceptual models appear reasonable, although for different ranges of flux as described below.

Under semi-arid climatic conditions, with estimates of average flux through the mountain on the order of 0.1 mm/yr or less, the flow of liquid water would be dominated by flow through the rock matrix and it may be possible to represent it as 1-D, vertical, downward flow. If the flow were in fact 1-D, then performance assessment analyses could be greatly simplified. In this conceptual model, as long as conditions are isothermal, all of the water that percolates past the zone where evapotranspiration occurs ultimately passes through the repository horizon and flows down to the water table.

The existence of sharp permeability contrasts and fault zones may cause flow to be diverted down-dip

either below or above the repository horizon toward or into the fault zones. This may be especially true at higher fluxes (approximately 1.0 mm/yr or greater) where flow in fractures might be expected to predominate over flow through the rock matrix. Water diverted below the repository from the bulk rock into the fault zones would have passed through the repository and would be carrying leached radionuclides. This diverted water might reach the water table relatively quickly and have a detrimental effect on repository performance. If water is diverted above the repository horizon, the amount of water available to contact waste packages and leach radionuclides could be significantly less than the average recharge rates might indicate. Such a diversion of water could greatly benefit the performance of the waste packages. Also, a repository could be designed so that water diverted into the faults above the repository would never come into contact with any waste packages.

To do performance assessment analyses efficiently, it is necessary to distinguish the conditions that would or would not give rise to lateral diversion of flow. Then analysis methods that are appropriate for the chosen conceptual model may be applied.

Six base cases are defined below: four for the 1-D flow model and two for the 2-D flow model. Analyses of both steady and nonsteady flow are suggested for the 1-D cases. With currently available analytical techniques, it is expected to be very costly to perform analyses of nonsteady flow that start from a well-characterized steady-flow state, so only steady-flow analyses are suggested at this time for the 2-D cases.

Mathematical Model for Partially Saturated Flow in a Compressible, Fractured Tuff

The model for partially saturated flow in a compressible medium that is suggested for these analyses has been described in detail by Klavetter and Peters, 1986. This highly nonlinear model uses a composite continuum approach to describe the effective hydrologic properties of the fractured rock mass. The model is cast with pressure head, ψ , as the primary variable. Klavetter and Peters, 1986, list the following important assumptions used in the derivation of the flow equations presented here:

1. The continuity equation for the matrix grain mass

2. The three-dimensional bulk-rock-consolidation equation with only vertical displacement (Reeves and Duguid, 1975)
3. The assumption that a unit change in the quantity "total saturation times pressure head" at a point causes a unit change in the local stress field (McTigue, Wilson, and Nunziato, 1984)
4. Darcy's equation for flow
5. Identical pressure head in the fractures and the matrix in the direction perpendicular to flow
6. Total head defined as the sum of pressure head and the elevation above some reference surface

The equations and definitions of variables are given below. The same mathematical model is applicable to the conceptual models for both 1-D and 2-D flow. The derivation of this mathematical model is tailored specifically for the problem of partially saturated flow in layered, fractured tuffs. The complete derivation with discussion of the assumptions can be found in Klavetter and Peters, 1986.

Saturation

Saturation, S , is a nonlinear function of the pressure head, ψ . The functional form of the relationship suggested for these analyses is that developed by van Genuchten, 1978.

$$S = (S_s - S_r) \left\{ \frac{1}{1 + |\alpha\psi|^\beta} \right\}^\lambda + S_r, \quad \psi \leq 0 \quad (1)$$

$$S = S_s \approx 1.0 \quad \psi \geq 0$$

where $\lambda = 1 - 1/\beta$. In the equations that follow, the matrix saturation, S_m , and fracture saturation, S_f , are calculated using Equation 1.

Hydraulic Conductivity

Van Genuchten's relationship for saturation can be used with the method developed by Mualem, 1976, to develop an analytical expression for hydraulic conductivity, K , as a function of pressure head, ψ . This yields the following equation:

$$K(\psi) = K_s [1 + |\alpha\psi|^\beta]^{-\frac{\lambda}{2}} \left\{ 1 - \left[\frac{|\alpha\psi|^\beta}{1 + |\alpha\psi|^\beta} \right]^\lambda \right\}^2, \quad \psi \leq 0 \quad (2)$$

$$K(\psi) = K_s, \quad \psi \geq 0$$

where $\lambda = 1 - 1/\beta$. In the equations that follow, the hydraulic conductivity tensors $\bar{K}_{m,b}$ and $\bar{K}_{f,b}$ (bulk

conductivities for the matrix and fractures respectively) are calculated using Equation 2. When calculating bulk conductivities, K_s in Equation 2 assumes the value of the bulk saturated conductivity given later in Table 3.

Nonsteady-Flow Equation

The following nonlinear equation can be used to describe water flow under nonsteady conditions:

$$\begin{aligned} \rho \frac{\partial \psi}{\partial t} \left\{ n_m \frac{\partial S_m}{\partial \psi} + n_f \frac{\partial S_f}{\partial \psi} + \beta_w (S_m n_m + S_f n_f) \right. \\ \left. + \alpha'_{bulk} \left[\frac{S_m n_m + S_f n_f}{n_m + n_f} \right] [S_m - n_f (S_m - S_f)] \right. \\ \left. - \frac{\partial n_f}{\partial \sigma'} \left[\frac{S_m n_m + S_f n_f}{n_m + n_f} \right] (S_m - S_f) \right\} \\ = \nabla \cdot \{ \rho (\bar{K}_{m,b} + \bar{K}_{f,b}) \cdot \nabla (\psi + z) \} \quad (3) \end{aligned}$$

This mathematical model for nonsteady, partially saturated flow includes the effects of the compressibilities of water and of the bulk rock mass. Including these effects makes the equation both more correct physically and, for some of the hydrogeologic units, more stable numerically. In this formulation of the mathematical model, compressibility effects are included as capacitance coefficients. Klavetter and Peters, 1986, defined five components in the capacitance term. These components are given in Equations 4 through 8. The five capacitance coefficients have been evaluated using base-case parameters and are shown graphically in Appendix A (Figures A1 through A6) for each of the hydrogeologic units.

$$\text{Matrix Sat.: } n_m \frac{\partial S_m}{\partial \psi} \quad (4)$$

$$\text{Fracture Sat.: } n_f \frac{\partial S_f}{\partial \psi} \quad (5)$$

$$\text{Water Comp.: } \beta_w (S_m n_m + S_f n_f) \quad (6)$$

$$\begin{aligned} \text{Bulk Rock Comp.:} \\ \alpha'_{bulk} \left[\frac{S_m n_m + S_f n_f}{n_m + n_f} \right] [S_m - n_f (S_m - S_f)] \approx \alpha'_{bulk} S_m^2 \quad (7) \end{aligned}$$

$$\begin{aligned} \text{Fracture Comp.:} \\ \frac{\partial n_f}{\partial \sigma'} \left[\frac{S_m n_m + S_f n_f}{n_m + n_f} \right] (S_m - S_f) \approx \frac{\partial n_f}{\partial \sigma'} S_m (S_m - S_f) \quad (8) \end{aligned}$$

The capacitance coefficients shown above were derived from fundamental relationships among porosity, n , saturation, S , water density, ρ , pressure head, ψ , and effective stress, σ' . The effects of compressibility of water and the bulk rock mass could also be incorporated into the model by explicitly retaining the fundamental relationships among pressure head, effective stress, porosity, and saturation rather than by using the derived capacitance coefficients.

Steady-Flow Equation

The steady-state version of the flow equation is also taken from Klavetter and Peters, 1986:

$$-(\bar{K}_{m,b} + \bar{K}_{f,b}) \cdot \nabla(\psi + z) = \bar{q}_m + \bar{q}_f = \bar{q}_{total} \quad (9)$$

Flow Velocity of Water

The following formulation can be used to calculate the average linear flow velocities of water in the matrix, \bar{v}_m , and fractures, \bar{v}_f . The average water velocity is the Darcy flux, \bar{q} , divided by the area through which the water moves. It is assumed that the water present at residual saturation does not contribute to the effective flow area. This formulation is taken from Peters, Gauthier, and Dudley, 1986.

$$\begin{aligned} \bar{v}_m &= \frac{\bar{q}_m}{n_m(S_m - S_{m,r})} \\ &= -\bar{K}_{m,b} \cdot \nabla(\psi + z) \left\{ \frac{1}{n_m(S_m - S_{m,r})} \right\} \end{aligned} \quad (10)$$

$$\begin{aligned} \bar{v}_f &= \frac{\bar{q}_f}{n_f(S_f - S_{f,r})} \\ &= -\bar{K}_{f,b} \cdot \nabla(\psi + z) \left\{ \frac{1}{n_f(S_f - S_{f,r})} \right\} \end{aligned} \quad (11)$$

Numerical-Convergence Criteria

The combined nonlinearities of the mathematical model and of the hydrologic properties for unsaturated tuff make it difficult to achieve numerical results that are stable and accurate. In calculations similar to these (Bixler and Eaton, 1986, and Peters, Gauthier, and Dudley, 1986), it has been observed that predicted pressures are relatively insensitive measures of calculational error. Velocities, on the other hand, are relatively good measures of error for these analyses because they are very sensitive to small perturbations in the pressure field. This mathematical model is cast so that pressure head, ψ , is the primary variable. A very strict convergence criterion must be applied to ψ to ensure reasonable accuracy in calculated velocities, \bar{v} ,

and fluxes, \bar{q} (see Bixler and Eaton, 1986, for an example).

Sensitivity Analyses for 1-D Flow

Description

In the conceptual model for 1-D flow, it is assumed that all moisture that infiltrates past the zone of evapotranspiration flows vertically downward to the water table. In this model, it is assumed that, at all fluxes being considered, the existence of the following conditions are not sufficient to cause water to be diverted laterally:

1. Anisotropic hydraulic conductivities
2. Conductivity contrasts at contacts between hydrogeologic units
3. Structural tilting of the hydrogeologic units
4. Distortions of the flow field caused by the presence of major structural features having hydraulic properties that are different from those of the surrounding rock mass

The vertical column for the 1-D base cases is shown in Figure 2. It is made up of five distinct, effectively horizontal, hydrogeologic units. The lowermost unit may be made up of either vitric or zeolitic materials (Ev or Ez). Assume that the repository is located in the welded tuffs of Unit D. Coordinates for the locations numbered in Figure 2 are listed in Table 2.

The overall height of the modeled column is 530.4 m. In the column being modeled, the water table, defined as the point at which $\psi = 0.0$ m, is located in Unit E. Since the purpose of these analyses is to test the sensitivity of model outputs (i.e., the performance measures) to variations in the parameters for the zone of partially saturated flow, the water table is taken as the lower boundary of the modeled region. The water table is also taken as the reference datum, $z = 0.0$ m. A known flux, \bar{q} , is applied at the upper boundary, $z = 530.4$ m. Temperature conditions are isothermal. It is assumed that the presence of the repository does not affect the hydrologic properties of Unit D, so the properties of Unit D are taken to be uniform from elevation $z = 130.3$ m to $z = 335.4$ m. In the base case, Unit E consists of all zeolitized material (Ez). Each unit is initially assumed to be homogeneous and isotropic.

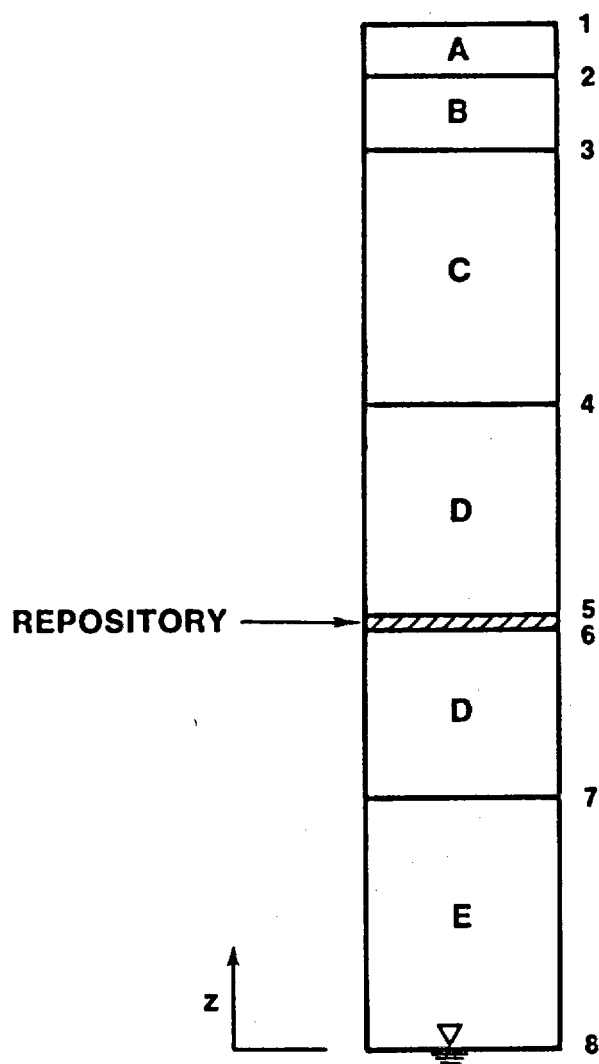


Figure 2. Stratigraphy for 1-D Base Cases (Cases 1 through 4)

Table 2. Coordinates of the Numbered Points for the 1-D Flow Analyses (see Figure 2)

Point	Elevation, z (m)
1	530.4
2	503.6
3	465.5
4	335.4
5	224.0
6	219.5
7	130.3
8	0.0

Performance Measures

Performance measures are defined for both the steady- and nonsteady-flow cases.

Steady Flow

The performance measure for the 1-D steady-flow calculations is the shortest water travel time between the base of the repository and the water table. We note that for most HYDROCOIN participants, the flux of water is of more importance to performance assessments than the water travel time. However, since the flow is 1-D, isothermal, and steady-state, the flux throughout the entire column is prescribed by the flux applied at the upper boundary. The volumetric rate of flow through the repository horizon is thus determined by the problem specification. Therefore, volumetric rate of water flow through the repository, though it is a good indicator of calculational stability and accuracy, is not a meaningful measure of sensitivity for the 1-D, steady-flow cases.

In steady-state analyses, water travel time is a function of the flux and of the effective volume of water along the flow path. The effective water volume is in turn a nonlinear function of pressure head, ψ . Thus, the travel time is a nonlinear function of all of the parameters that affect the distribution of moisture and pressure head in the column, Equations 1, 2, and 9, and can be used as a performance measure to test the sensitivity of the mathematical model to these parameters.

Nonsteady Flow

The first performance measure for the 1-D, nonsteady-flow cases is again taken to be the shortest water travel time between the base of the repository and the water table. In these analyses, it is assumed that the change in infiltration rate at the upper boundary occurs when radionuclides are first released from the repository. The flux pulse will then overrun water that has already passed through the repository under the influence of the initial steady-state flux conditions. Therefore, travel time from the repository should be calculated starting at the time the upper boundary condition is changed to the new infiltration rate.

The second and third performance measures are, respectively, the time-dependent normalized volume of flow passing the base of the repository, $z = 219.5$ m, and the normalized volume of flow passing the water table, $z = 0.0$ m. The flow volume at any time, t , is to be calculated for a 1.0-m^2 flow area and is to be normalized by the initial flow volume, $\bar{q}(t)/\bar{q}(t_0)$.

Criterion for Nonnegligible Flow Volume

The calculation of the minimum water travel time from the repository to the water table will be based on the greater of the velocity of flow in the fractures, v_f , or in the rock matrix v_m . The volume of water flowing at the higher velocity must be a significant portion of the total volume of flow; otherwise the travel time would not be a meaningful performance measure. It is expected that, under some conditions, the calculated velocity of water flowing in the fractures will be much higher than the velocity in the rock matrix, while the volume of water flowing through the fractures will be negligible by comparison with the volume flowing through the matrix. To ensure that small volumes of water flowing at relatively high velocity in the fractures do not inappropriately dominate the calculation of minimum travel times, the following cut-off criterion should be applied: if v_f is greater than v_m , use v_f to calculate the minimum travel time only if $q_f/q_{\text{total}} \geq 10^{-3}$.

Base-Case Parameters

For local sensitivity analyses, a base-case analysis determines the point in parameter space at which model sensitivities are tested. Because of the extremely nonlinear nature of this problem, sensitivities are expected to be dependent on the flux chosen for the base cases. For this reason, two base cases each are proposed for steady and nonsteady analyses. For steady-flow conditions, the base-case fluxes are

Case 1: $q = 0.1$ mm/yr for matrix-dominated flow

Case 2: $q = 1.0$ mm/yr for conditions near the transition from matrix-dominated to fracture-dominated flow

For the nonsteady-flow cases, it is assumed that steady-flow conditions prevail under the initial flux and then a step change in flux is applied. Nonsteady flow is then observed until a new steady-flow condition is reached. For nonsteady-flow conditions, the base-case fluxes are

Case 3: q changes from 0.1 mm/yr to 0.2 mm/yr for nonsteady, matrix-dominated flow

Case 4: q changes from 0.5 mm/yr for nonsteady flow in the transition from matrix-dominated to combined matrix and fracture flow

Base-case values for the hydrologic properties are given in Table 3 for each of the hydrogeologic units. The base-case value for each parameter is given first and then, for those parameters to be varied, a suggested range of values to use for sensitivity analyses is given below it in parentheses. Base-case capacitance coefficients calculated from Equations 4 through 8 are displayed graphically in Appendix A, Figures A1 through A6, for each of the hydrogeologic units included in these analyses. The base-case hydraulic conductivities for each unit are plotted in Appendix A, Figures A7 through A12. Calculations using parameters similar to these have been reported by Peters, Gauthier, and Dudley, 1986, and Dudley et al., in preparation.

Table 3. Base-Case Values and Ranges of Properties for the Hydrologic Units in the Unsaturated Zone of the Tuff Site

Compressibility Factors

The compressibility of water, β_w , is $9.8E-7/m$.

Unit	A	B	C	D	Ev	Ez
Coefficient of Consolidation [a]	6.2	82.	12.	5.8	39.	26.
α'_{bulk} ($1.E-7/m$)	(0.1-50)	(10-250)	(0.1-50)	(0.1-50)	(1-150)	(1-150)

Matrix Properties [b]

Unit	Grain Density (g/cm^3)	Porosity n_m	Saturated Hydraulic Conductivity, $K_{m,b}$ (m/s) [c]	Residual Saturation, S_r	Alpha α ($1/m$)	Beta β
A	2.49	0.08 (0.05-0.15)	9.7×10^{-12} $1.0 \times 10^{-13} - 5.0 \times 10^{-10}$	0.002 (0.00-0.18)	0.00821 (0.003-0.024)	1.558 (1.3- 2.4)
B	2.35	0.40 (0.20-0.70)	3.9×10^{-07} $1.0 \times 10^{-09} - 5.0 \times 10^{-05}$	0.100 (0.00-0.15)	0.01500 (0.001-0.031)	6.872 (1.2-15.0)
C	2.58	0.11 (0.05-0.20)	1.9×10^{-11} $1.0 \times 10^{-13} - 5.0 \times 10^{-10}$	0.080 (0.00-0.23)	0.00567 (0.001-0.020)	1.798 (1.2- 2.5)
D	2.58	0.11 (0.05-0.20)	1.9×10^{-11} $1.0 \times 10^{-13} - 1.0 \times 10^{-09}$	0.080 (0.00-0.32)	0.00567 (0.001-0.020)	1.798 (1.2- 2.5)
Ev	2.37	0.46 (0.30-0.55)	2.7×10^{-07} $1.0 \times 10^{-13} - 5.0 \times 10^{-06}$	0.041 (0.00-0.25)	0.01600 (0.005-0.060)	3.872 (1.3- 7.0)
Ez	2.23	0.28 (0.20-0.45)	2.0×10^{-11} $1.0 \times 10^{-14} - 5.0 \times 10^{-10}$	0.110 (0.00-0.30)	0.00308 (0.001-0.030)	1.602 (1.2- 3.5)

Notes: a) Based on Nimick, *et al.*, 1984.

b) All base-case matrix data in this section are from Peters *et al.*, 1984.

c) The matrix saturated conductivity and the bulk matrix saturated conductivity ($K_{m,b}$) are essentially the same because the factor that converts the matrix value to the bulk matrix value, $(1-n_p)$, is nearly equal to one.

(continued)

Table 3. concluded

Unit	Fracture Properties [d]				
	Horizontal Stress [e] (bars)	Fracture Aperture (microns)	Saturated Fracture Hydraulic Conductivity (m/s)	Fracture Density [f] (no./m ³)	Fracture Porosity [g] n_f
A	1.1	6.74	3.8×10^{-5} $5.0 \times 10^{-7} - 5.0 \times 10^{-3}$	20	1.4×10^{-4} $1.0 \times 10^{-5} - 1.0 \times 10^{-3}$
B	3.3	27.0	6.1×10^{-4} $5.0 \times 10^{-6} - 5.0 \times 10^{-2}$	1	2.7×10^{-5} $2.0 \times 10^{-6} - 2.0 \times 10^{-4}$
C	9.5	5.13	2.2×10^{-5} $5.0 \times 10^{-7} - 1.0 \times 10^{-3}$	8	4.1×10^{-5} $2.0 \times 10^{-6} - 1.0 \times 10^{-3}$
D	21.9	4.55	1.7×10^{-5} $1.0 \times 10^{-7} - 1.0 \times 10^{-3}$	40	1.8×10^{-4} $1.0 \times 10^{-5} - 5.0 \times 10^{-3}$
Ev	34.3	15.5	2.0×10^{-4} $2.0 \times 10^{-6} - 2.0 \times 10^{-2}$	3	4.6×10^{-5} $5.0 \times 10^{-6} - 5.0 \times 10^{-4}$
Ez	34.3	15.5	2.0×10^{-4} $2.0 \times 10^{-6} - 2.0 \times 10^{-2}$	3	4.6×10^{-5} $5.0 \times 10^{-6} - 5.0 \times 10^{-4}$

Unit	Bulk Fracture				
	Fracture Compressibility (1/m)	Saturated Hydraulic Conductivity [h] K_{fb} (m/s)	Residual Saturation, S_r	Alpha α (1/m)	Beta β
A	1.3×10^{-6} $1.0 \times 10^{-7} - 1.0 \times 10^{-5}$	5.3×10^{-9} $5.0 \times 10^{-12} - 5.0 \times 10^{-6}$	0.0395 (0.00–0.15)	1.2851 (0.2–6.0)	4.23 (1.2–7.0)
B	1.9×10^{-7} $2.0 \times 10^{-8} - 2.0 \times 10^{-6}$	1.6×10^{-8} $1.0 \times 10^{-11} - 1.0 \times 10^{-5}$	0.0395 (0.00–0.15)	1.2851 (0.2–6.0)	4.23 (1.2–7.0)
C	5.6×10^{-8} $6.0 \times 10^{-9} - 6.0 \times 10^{-7}$	0.9×10^{-9} $1.0 \times 10^{-12} - 1.0 \times 10^{-6}$	0.0395 (0.00–0.15)	1.2851 (0.2–6.0)	4.23 (1.2–7.0)
D	1.2×10^{-7} $1.0 \times 10^{-8} - 1.0 \times 10^{-6}$	3.1×10^{-9} $1.0 \times 10^{-12} - 5.0 \times 10^{-6}$	0.0395 (0.00–0.15)	1.2851 (0.2–6.0)	4.23 (1.2–7.0)
Ev	2.8×10^{-8} $3.0 \times 10^{-9} - 3.0 \times 10^{-7}$	9.2×10^{-9} $1.0 \times 10^{-11} - 1.0 \times 10^{-5}$	0.0395 (0.00–0.15)	1.2851 (0.2–6.0)	4.23 (1.2–7.0)
Ez	2.8×10^{-8} $3.0 \times 10^{-9} - 3.0 \times 10^{-7}$	9.2×10^{-9} $1.0 \times 10^{-11} - 1.0 \times 10^{-5}$	0.0395 (0.00–0.15)	1.2851 (0.2–6.0)	4.23 (1.2–7.0)

Notes: d) Unless otherwise noted, base-case fracture information is based on Peters *et al.*, 1984.
e) Horizontal stress is assumed to be one-third of the overburden weight, evaluated at the average unit depth.
f) Based on Scott *et al.*, 1983.
g) Calculated as fracture volume (aperture times 1 m²) times the number of fractures per cubic meter.
h) This value of K_{fb} was obtained by multiplying the fracture conductivity by the fracture porosity.

Variations

To make good decisions about the amount and quality of data required to properly support the use of a particular mathematical model, it is necessary to test the sensitivity of that model to the parameters involved to determine which parameters are most important. The following paragraphs suggest variations for parameters for which sensitivities of the 1-D model for partially saturated flow in fractured tuff should be investigated.

Estimates of the flux under semiarid climatic conditions and possible fluxes that could result from a change to a wetter climate vary widely. For the steady-flow analyses, two ranges of flux should be considered:

1. $0.01 \text{ mm/yr} \leq \bar{q} \leq 0.5 \text{ mm/yr}$ for base case 1 with $\bar{q} = 0.1 \text{ mm/yr}$
2. $0.50 \text{ mm/yr} \leq \bar{q} \leq 4.0 \text{ mm/yr}$ for base case 2 with $\bar{q} = 1.0 \text{ mm/yr}$

Saturated hydraulic conductivities for both matrix and fractures have significant natural variability within each hydrogeologic unit. The low measured conductivities are also subject to experimental errors. Possible ranges for the saturated conductivities for each unit are listed in Table 3. Uncertainty in these values is not expected to be correlated between units.

A further uncertainty in the hydraulic conductivity values is introduced by the model being used to relate pressure head, degree of saturation, and conductivity for conditions of partial saturation and by the experimental techniques used to estimate the parameters for that model. Neither the model nor the experimental techniques have been validated for welded or nowelded, fractured tuffs. Possible ranges for residual saturation, S_r , and the modeling parameters α and β are suggested in Table 3.

Matrix and fracture porosities are known to be highly variable. The distributions of matrix porosities are moderately well known, but the distributions of fracture porosities are poorly known. Currently available data suggest that there is no direct correlation between porosity and hydraulic conductivity. Possible ranges of porosity for sensitivity analyses are listed in Table 3.

Water travel time from the repository to the water table is nonlinearly related to the location of the water table because of the dependence of the moisture distribution on the lower boundary condition. A climate change could raise the level of the water table and shorten the water travel time from the repository to the accessible environment. For these analyses, the water table could be considered to rise anywhere from 0.0 m to 20.0 m above its current elevation.

Portions of Unit E in the unsaturated zone have been thermally and chemically altered from their original vitric form (Ev) to a zeolitized form (Ez). The relative thicknesses of vitric and zeolitic materials vary across the repository site. Any given column could contain all vitric material, all zeolitic material, or any combination in between these two extremes. Whenever both forms are present, the vitric materials (Ev) always overlie the zeolitic materials (Ez). Because saturated hydraulic conductivities of the matrix material in the zeolitic form (Ez) are several orders of magnitude lower than in the vitric form (Ev), water travel time could be very sensitive to the thickness of each material in the geologic column.

Sensitivity Analyses for 2-D Flow

Description

Montazer and Wilson, 1984, suggested that both the bedding within nonwelded units and the sharp contrast in hydraulic conductivities at contacts between welded and nonwelded units could give rise to a significant amount of lateral flow. In the proposed 2-D analyses, all of the factors that could cause lateral flow are allowed to act. As in the conceptual model for 1-D flow, it is assumed that the flux entering the top of the column has already migrated past the zone of evapotranspiration.

The hydrogeologic units involved in the conceptual model for 2-D flow are those previously described in Table 1. Figure 3 shows the geologic section for these analyses. The earlier 1-D column has simply been expanded to a 2-D section and the units have been tilted to an average dip of 6° . The dip of the units ranges from 5° to 8° . The modeled region is bounded on the right by a fault zone, and it is assumed that the repository extends across the fault zone. The overall height of the modeled section is 635.5 m; the width is 1000.0 m. Coordinates for the locations numbered in Figure 3 are listed in Table 4.

Each unit is taken to be homogeneous and isotropic. A known vertical flux, \bar{q} , is applied along the upper boundary. The left boundary, $x = 0.0 \text{ m}$, is a no-flow boundary; the fault zone along the right boundary, $x = 1000.0$ to 1000.5 m , is also initially taken to be represented by a no-flow boundary at $x = 1000.0 \text{ m}$. The water table, $\psi = 0.0 \text{ m}$ at $z = 0.0 \text{ m}$, is again taken as the lower boundary of the modeled region; it is located within Unit E and is assumed to be horizontal. Temperature conditions are isothermal.

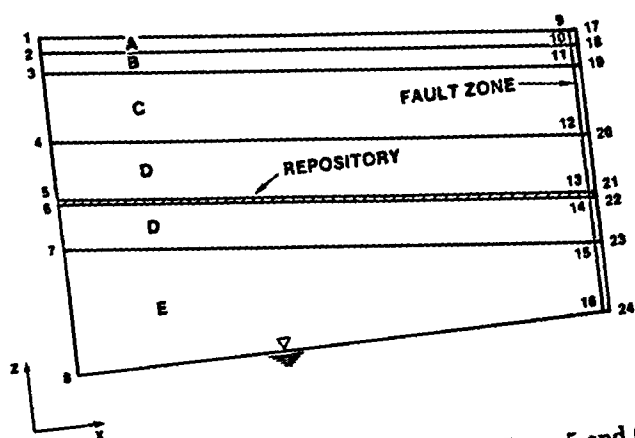


Figure 3. Stratigraphy for 2-D Base Cases (Cases 5 and 6)

Table 4. Coordinates of the Numbered Points for the 2-D Flow Analyses (see Figures 3 and 4)

Point	Coordinates (m)	
	x	z
1	0.0	635.5
2	0.0	608.7
3	0.0	570.6
4	0.0	440.5
5	0.0	329.1
6	0.0	324.6
7	0.0	235.4
8	0.0	0.0
9	1000.0	530.4
10	1000.0	503.6
11	1000.0	465.5
12	1000.0	335.4
13	1000.0	224.0
14	1000.0	219.5
15	1000.0	130.3
16	1000.0	0.0
17	1000.5	530.4
18	1000.5	503.6
19	1000.5	465.5
20	1000.5	335.4
21	1000.5	224.0
22	1000.5	219.5
23	1000.5	130.3
24	1000.5	0.0

Simplified 2-D Analyses

Because of the computational requirements involved in attempting to analyze the entire five-layer, two-dimensional section, some HYDROCOIN teams may prefer to attempt a simplified section consisting either of the upper three layers (Units A, B, and C) or of the lower three layers (Units C, D, and E). All of the phenomena of interest can be observed in these layers. The stratigraphies for these simplified sections should be as shown in Figure 4. Coordinates of the numbered locations are the same as those listed in Table 4.

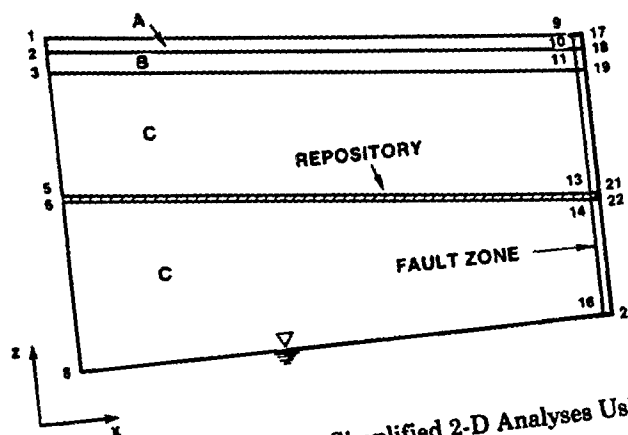


Figure 4a. Stratigraphy for Simplified 2-D Analyses Using Units A, B, and C

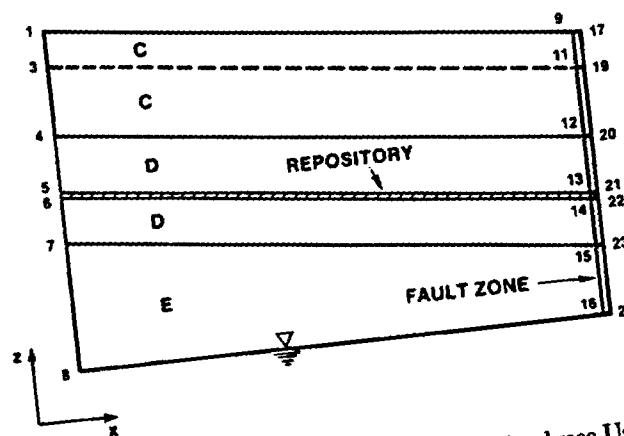


Figure 4b. Stratigraphy for Simplified 2-D Analyses Using Units C, D, and E

If the upper three layers are analyzed, Unit C should be extended downward to the water table, Figure 4a. Naturally, if this section is chosen, no conclusions can be drawn regarding the flow conditions below the repository, and the representation of the conditions between the top of Unit D and the repository are only approximate.

If the lower three layers are analyzed, the infiltration boundary condition can be applied at the top of Unit C, dashed line in Figure 4b, or Unit C could be extended upward to the original infiltration surface, solid lines in Figure 4b. In either case, no conclusions can be drawn regarding the flow conditions above the top of Unit C. Also, any conclusions about flow through Units C, D, and E are conditioned by the fact that any lateral diversion of flow caused by Units A and B is ignored.

It may be possible to construct a global sensitivity analysis from separate "global" analyses of the two simplified sections. Construct input parameter vectors as if the entire five-layer section were to be analyzed. Use the same vectors for analyses of both the upper and lower sections; parameters for Unit C will be common to vectors used in both sets of analyses. When performing the analyses of the lower simplified section, take the pressure head and flux conditions at the top of Unit C from corresponding analyses of the upper three layers and apply them as boundary conditions at the top of Unit C. Then, by matching cases with the same input parameter vectors, recouple the separate analyses to draw conclusions regarding the global sensitivity of the entire five-layer system. Check the validity of this approach by analyzing a few cases with the full five-layer section.

Performance Measures

Performance measures for the 2-D flow cases are intended to assess the magnitude of lateral diversion of flow and its effect on the performance of the repository. The first measure is the spatial distribution of the volumetric flow rate of water passing through the repository horizon. There are two complementary flow rates that are of interest:

1. The flow rate of water moving through the bulk rock mass at the level of the repository
2. The flow rate of water diverted above the repository into the fault zone

All flow rates should be calculated for a 1.0-m thickness of the vertical section. This performance measure is applicable to analyses of the full five-layer section and to analyses of only the upper three layers.

The spatial distribution of water travel times from the base of the repository to the water table is the second performance measure. It will be interesting to observe what portion of the water flowing through the bulk rock mass at the level of the repository is diverted below the repository toward or into the fault zone and what effect this has on the distribution of water travel times. The criterion for nonnegligible flow volume that was described for the 1-D analyses also applies here. This performance measure is applicable to analyses of the full five-layer section and to analyses of only the lower three layers.

Base-Case Parameters

For the same reasons described previously for the 1-D flow analyses, two base-case fluxes are proposed for the 2-D, steady-flow analyses:

Case 5: $\bar{q} = 0.1$ mm/yr for matrix-dominated flow

Case 6: $\bar{q} = 1.0$ mm/yr for conditions near the transition from matrix-dominated to fracture-dominated flow

Base-case values for the hydrologic properties for each of the hydrogeologic units are those given in Table 3. No base-case values are given for hydrologic properties of the fault zone because the right boundary is being treated as a no-flow boundary in the base cases.

Variations

All of the variations suggested for the 1-D flow analyses also apply to the 2-D cases: changes in applied flux; saturated conductivities and parameters for conductivities for partially saturated flow; porosities; location of the water table; and relative proportions of vitric (Ev) and zeolitic (Ez) materials in Unit E. The two-dimensionality of these analyses introduces additional sources of uncertainty. Some of these are discussed below.

Little is known about the conditions at lateral boundaries or even what might be an appropriate boundary for site-scale analyses. In the base cases, the fault zone along the right boundary is treated as a no-flow boundary at $x = 1000.0$ m. It could also be modeled as a seepage face or as a column of fractured or unfractured, porous material between $x = 1000.0$ m and $x = 1000.5$ m. The right boundary of the column of porous material representing the fault can be taken as a no-flow boundary. The porous materials in the fault zone could have hydraulic conductivities that are

1. Slightly lower than those of the adjacent material from which they were derived
2. Comparable to those in the adjacent rock mass
3. Several orders of magnitude greater than those in the adjacent rock

In these variations, the saturated conductivities and parameters for partially saturated conductivities in the fault zone should be taken to be correlated with the properties of the parent rock. For simplicity, porosities in the fault zone will be taken to be identical to those of the adjacent rock mass.

It has been suggested that, when the nonwelded materials of Unit E are sheared at high confining stress, the hydrologic properties of the sheared material may be very similar to those of the intact rock. The result is that the fault zone may be hydraulically discontinuous through Unit E and may not act as an effective conduit for flow from the ground surface to the water table. To observe the effect this might have on the performance measures, allow the hydrologic properties of the fault zone through Units A, B, C, and D to vary as described in the previous paragraph while keeping the properties of the fault zone through Unit E the same as those of Unit E.

The effective width of materials in the fault zone having altered hydraulic properties is not known. For analyses with the fault modeled as a porous material, the width is initially taken to be 0.5 m and should be varied over a range of 0.1 to 3.0 m (0.0 to 3.0 m in Unit E).

Hydraulic conductivities were assumed to be isotropic in the 2-D base-case analyses. There is weak evidence that the effective, bulk, saturated conductivities of the various tuff units are anisotropic. The correlation between measured anisotropy in saturated conductivities and in conductivities for partially saturated flow is very poorly known. The magnitudes of the relative contributions to anisotropy from matrix and fractures are also uncertain. Ratios of horizontal to vertical conductivity could range from 0.1 to 1000. Here "horizontal" is taken to mean parallel to the dip of the hydrogeologic units and "vertical" is taken to mean perpendicular to dip. Anisotropy can be varied unit by unit, or the relative degree of anisotropy can be randomly selected for each unit.

Unit B, though primarily nonwelded, is assumed to contain numerous horizontal lenses of less-permeable welded materials. This heterogeneous unit could be modeled as a homogeneous unit with effectively anisotropic hydraulic conductivity. Because Unit B could intercept and divert water above the repository horizon, it may be particularly interesting

to investigate the sensitivity of the performance measures to anisotropy in this unit.

If there is a significant volume of water diverted above the repository from the rock mass into the fault zone, the volume of water contacting the waste could be reduced by not storing waste close to the fault. Consider truncating the repository 0.0 to 50.0 m to the left of the fault zone to observe the effect of the distance between the repository and the fault zone on the volumetric rate of water flow through the repository.

Mesh Design Considerations

Experience from analyses similar to those proposed in this paper indicates that results can be very sensitive to mesh design. Attention to mesh design is especially important in those parts of the problem domain having very steep hydraulic gradients.

Fine mesh zoning is needed where steep hydraulic gradients occur. If the mesh is too coarse, the steeper parts of the gradient may not be observed, and incorrect conclusions could be drawn about the flow conditions. For example, it has been observed in 1-D calculations that coarse gridding near layer boundaries, where there is a large contrast in hydraulic conductivity across the boundary, can lead to the appearance of perched water above the boundary. When the grid is further refined, the steepness of the hydraulic gradient is properly resolved, and water moves across the boundary without appearing to become perched.

Steep hydraulic gradients are typically observed at the boundaries between adjacent hydrologic units when there is a large contrast in hydraulic conductivity across the boundary. Also, in nonsteady analyses, saturation fronts moving through the problem domain create a moving zone with a steep gradient in the hydraulic conductivity because of large differences in saturation ahead of and behind the front. It is expected that steep conductivity gradients may also occur along the right boundary in the 2-D analyses. For an example of the steepness of the hydraulic gradients that can occur, see the analyses described by Peters, Gauthier, and Dudley, 1986.

Because of the wide range of values assigned to the hydrologic properties for these sensitivity analyses, it is not possible to state, in advance, where the steepest gradients will occur, since their location could change with each iteration. However, as previously mentioned, an ordinary differential equation (ODE) solver can be used to efficiently analyze 1-D, isothermal,

steady-state flow. When setting up any of the above analyses for finite-element or finite-difference codes, use of the ODE solver can help guide mesh design by identifying regions where very steep hydraulic gradients are likely to occur. An ODE solver can also be used to obtain reasonable estimates of initial conditions for steady-flow analyses.

References

- Bixler, N. E., and R. R. Eaton, 1986, "Sensitivity of Calculated Hydrological Flows Through Multilayered Hard Rock to Computational Solution Procedures," *Proceedings of the Symposium on Groundwater Flow and Transport Modeling For Performance Assessment of Deep Geologic Disposal of Radioactive Waste-A Critical Evaluation of the State of the Art*, Charles R. Cole, ed., Albuquerque, New Mexico.
- Dudley, A. L., et al., in preparation, "Total Systems Performance Assessment Code (TOSPAC) Volume 1: Physical and Mathematical Bases," SAND85-0002, Sandia National Laboratories, Albuquerque, New Mexico.
- Hodgkinson, D. P., et al., 1985, "Specification of a Test Problem for HYDROCOIN Level 3 Case 1: Sensitivity Analysis for Near-Surface Disposal in Argillaceous Media," AERE-R.11987, United Kingdom Atomic Energy Authority, AERE Harwell, Oxfordshire.
- Klavetter, E. A., and R. R. Peters, 1986, "Estimation of Hydrologic Properties for an Unsaturated, Fractured Rockmass," SAND84-2642, Sandia National Laboratories, Albuquerque, New Mexico.
- McTigue, D. F., R. K. Wilson, and J. W. Nunziato, 1984, "An Effective Stress Principle for Partially Saturated Media," SAND82-1977, Sandia National Laboratories, Albuquerque, New Mexico.
- Montazer, P., and W. E. Wilson, 1984, "Conceptual Hydrological Model of Flow in the Unsaturated Zone, Yucca Mountain, Nevada," Water-Resources Investigations Report 84-4345, U.S. Geological Survey, Lakewood, Colorado.
- Mualem, Y., 1976, "A New Model for Predicting the Hydraulic Conductivity of Unsaturated Porous Materials," *Water Resources Research*, vol. 12, no. 3, pp. 513-522.
- Nimick, F. B., S. J. Bauer, and J. R. Tillerson, 1984, "Recommended Matrix and Rockmass Bulk, Mechanical and Thermal Properties for Thermomechanical Stratigraphy of Yucca Mountain," Keystone Document 6310-85-1, Sandia National Laboratories, Albuquerque, New Mexico.
- Ortiz, T. S., et al., 1985, "A Three-Dimensional Model of Reference Thermal/Mechanical and Hydrological Stratigraphy at Yucca Mountain, Southern Nevada," SAND84-1076, Sandia National Laboratories, Albuquerque, New Mexico.
- Peters, R. R., J. H. Gauthier, and A. L. Dudley, 1986, "The Effect of Percolation Rate on Water-Travel Time in Deep, Partially Saturated Zones," SAND85-0854, Sandia National Laboratories; also in *Proceedings of the Symposium on Groundwater Flow and Transport Modeling For Performance Assessment of Deep Geologic Disposal of Radioactive Waste-A Critical Evaluation of the State of the Art*, Charles R. Cole, ed., Albuquerque, New Mexico, August 1986.
- Peters, R. R., et al., 1984, "Fracture and Matrix Hydrologic Characteristics of Tuffaceous Materials from Yucca Mountain, Nye County, Nevada," SAND84-1471, Sandia National Laboratories, Albuquerque, New Mexico.
- Reeves, M., and J. O. Duguid, 1975, "Water Movement Through Saturated-Unsaturated Porous Media: A Finite Element Galerkin Model," ORNL-4927, Oak Ridge National Laboratory, Oak Ridge, Tennessee.
- Scott, R. B., et al., 1983, "Geologic Character of Tuffs in the Unsaturated Zone at Yucca Mountain, Southern Nevada," in *Role of the Unsaturated Zone in Radioactive and Hazardous Waste Disposal*, J. Mercer, ed., Ann Arbor Science, Ann Arbor, Michigan.
- Van Genuchten, R., 1978, "Calculating the Unsaturated Hydraulic Conductivity with a new Closed Form Analytical Model," *Water Resources Bulletin*, Princeton University Press, Princeton University, Princeton, New Jersey.

APPENDIX A

Plots of Capacitance Coefficients and Hydraulic Conductivities

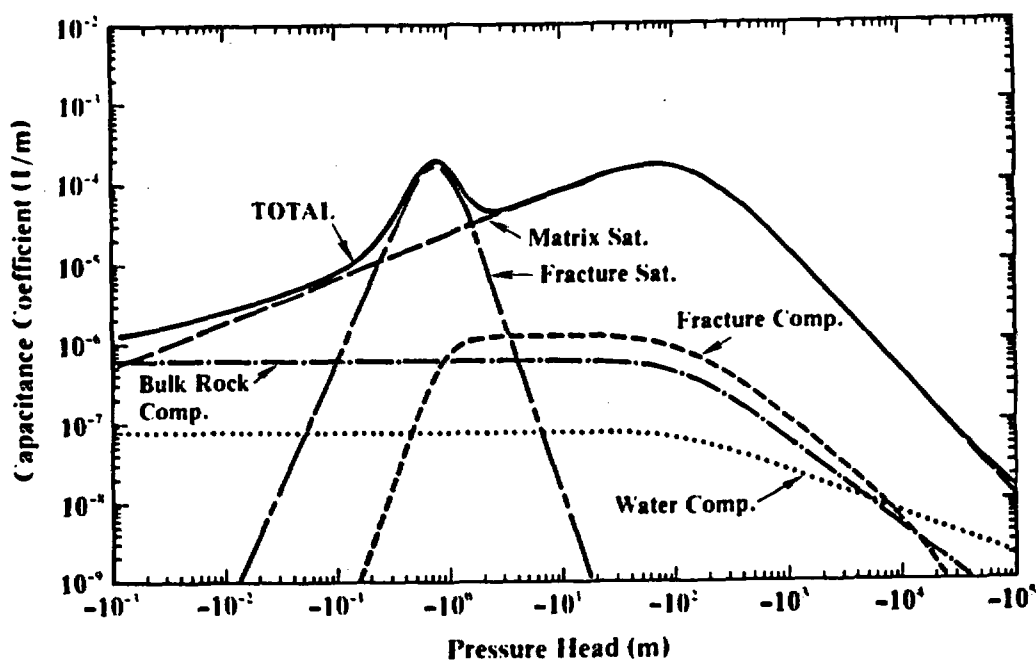


Figure A1. Capacitance Coefficients for Unit A

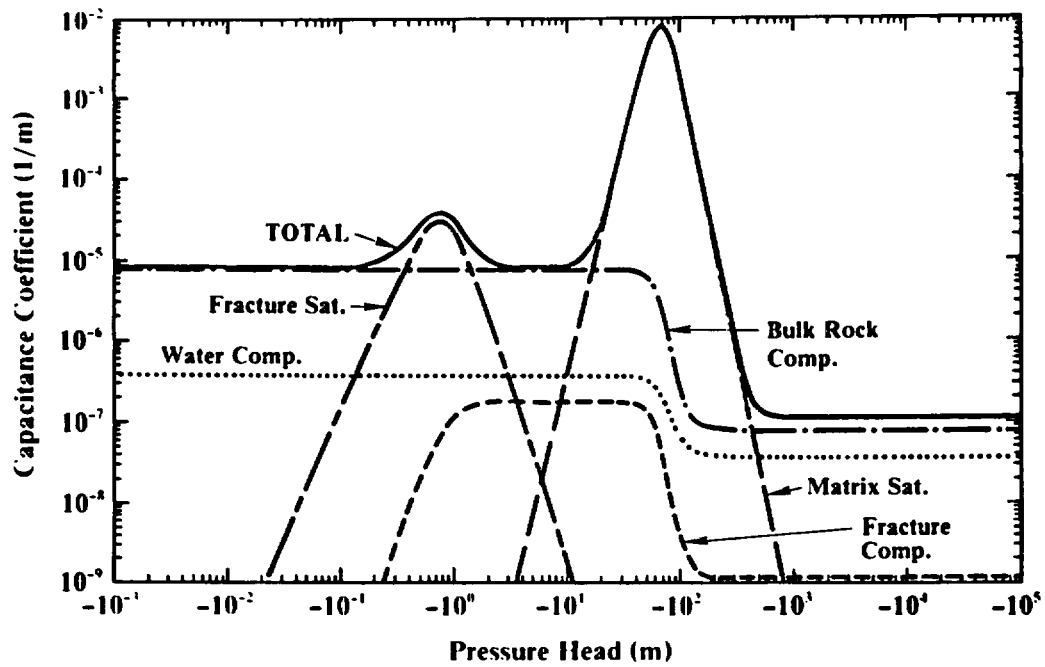


Figure A2. Capacitance Coefficients for Unit B

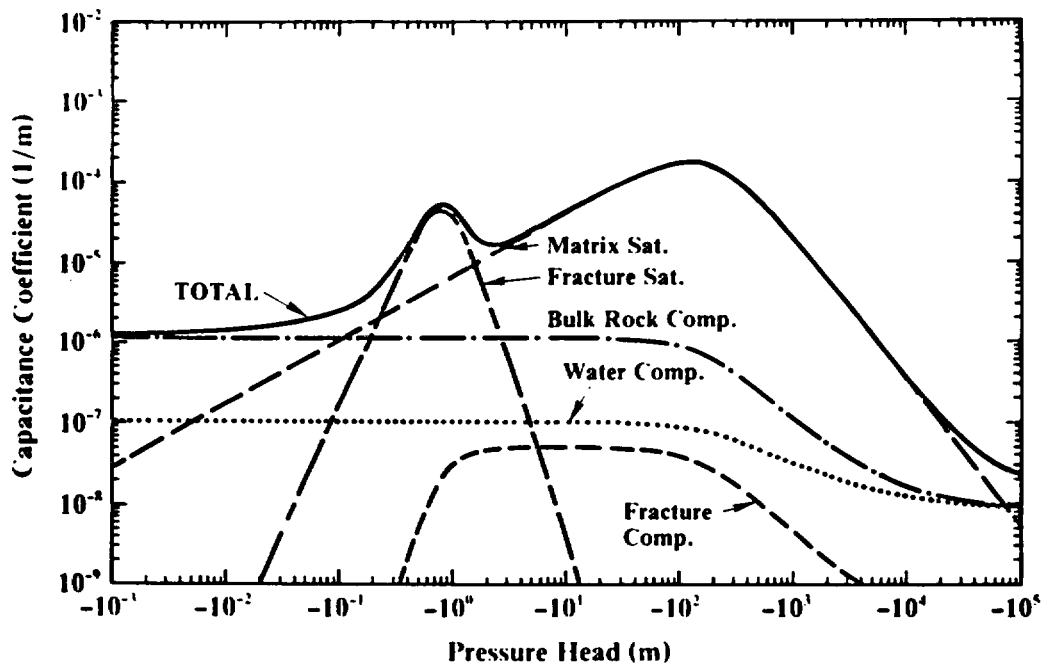


Figure A3. Capacitance Coefficients for Unit C

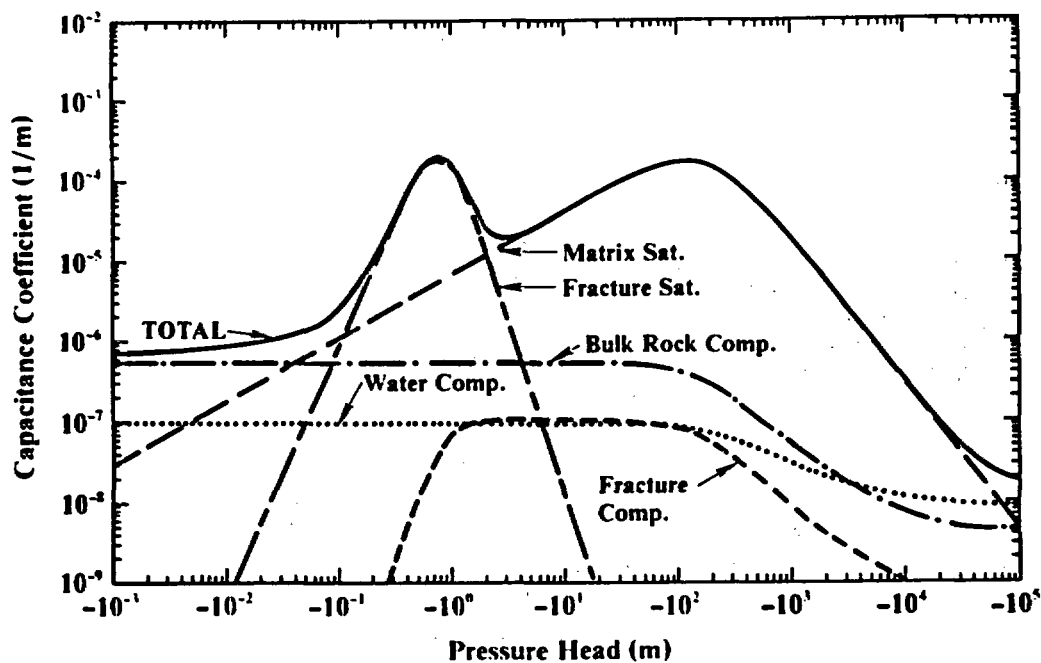


Figure A4. Capacitance Coefficients for Unit D

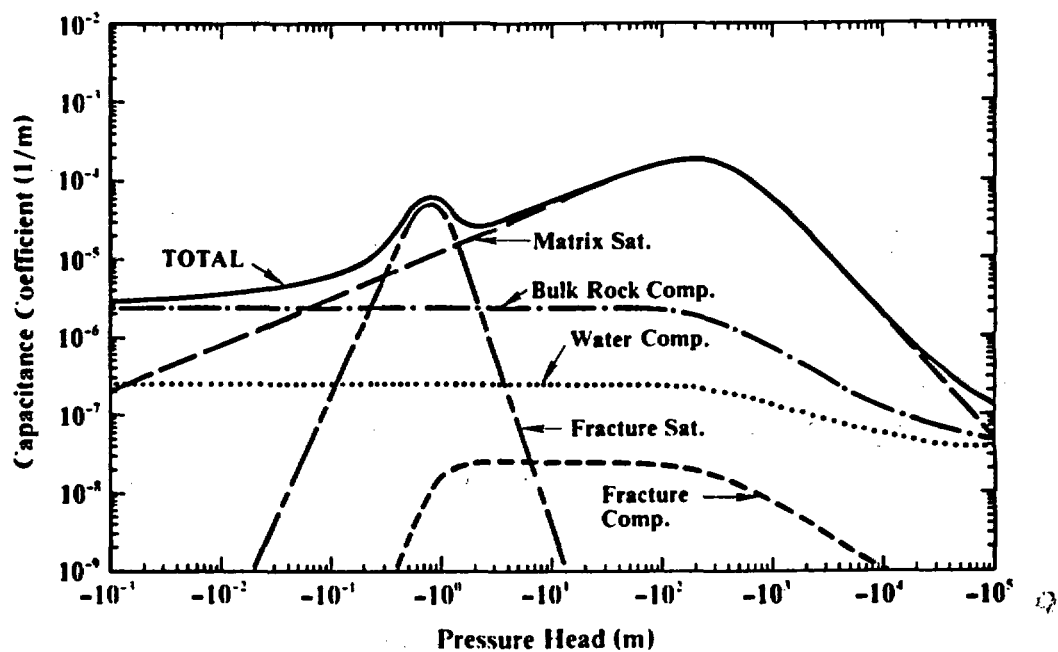


Figure A5. Capacitance Coefficients for Zeolitic Unit Ez

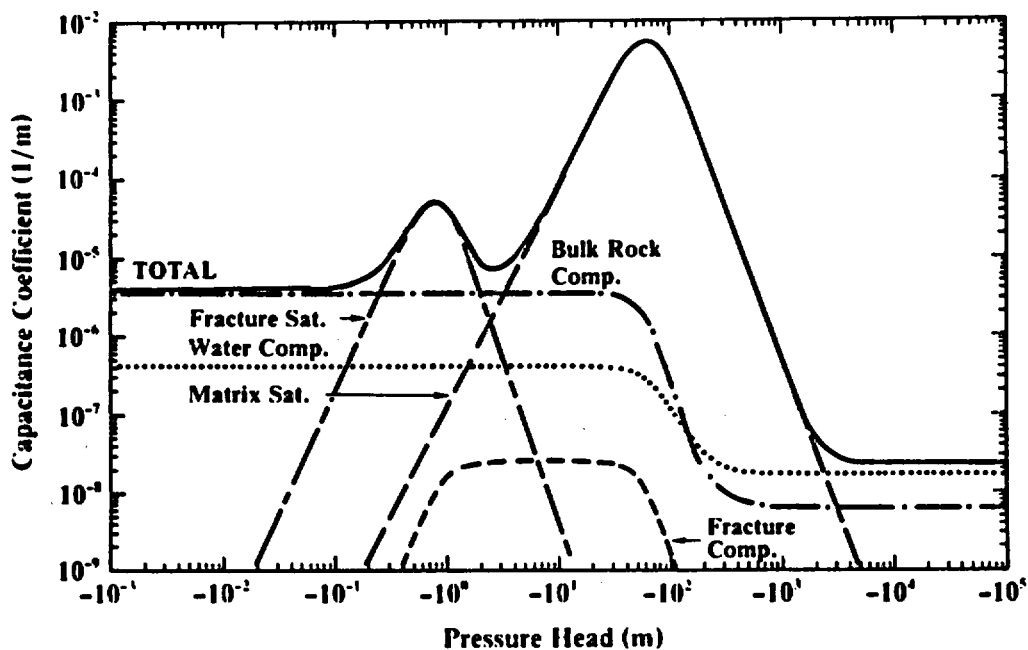


Figure A6. Capacitance Coefficients for Vitric Unit Ev

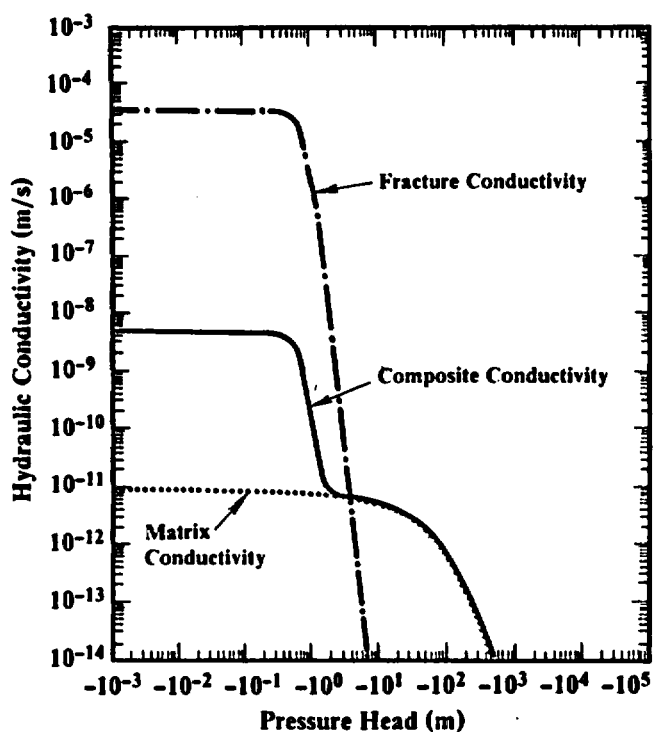


Figure A7. Hydraulic Conductivity Versus Pressure Head for Unit A

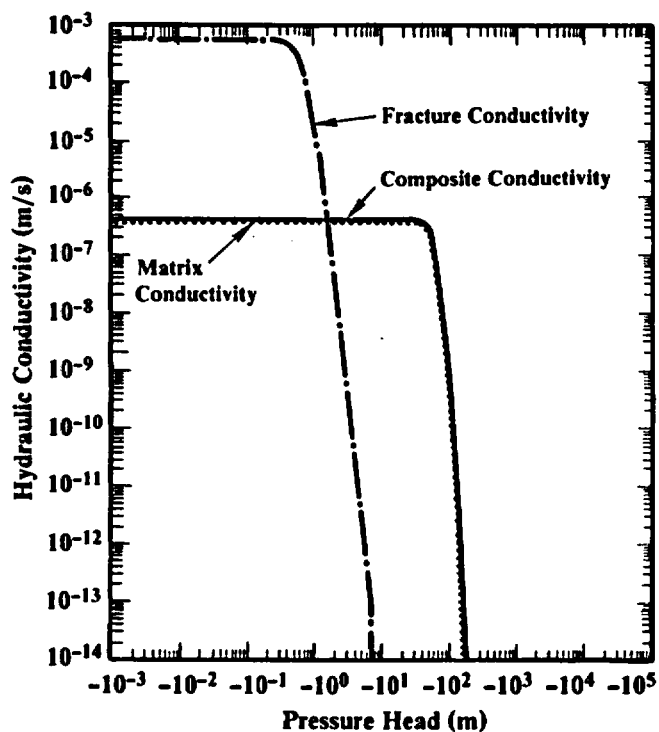


Figure A8. Hydraulic Conductivity Versus Pressure Head for Unit B

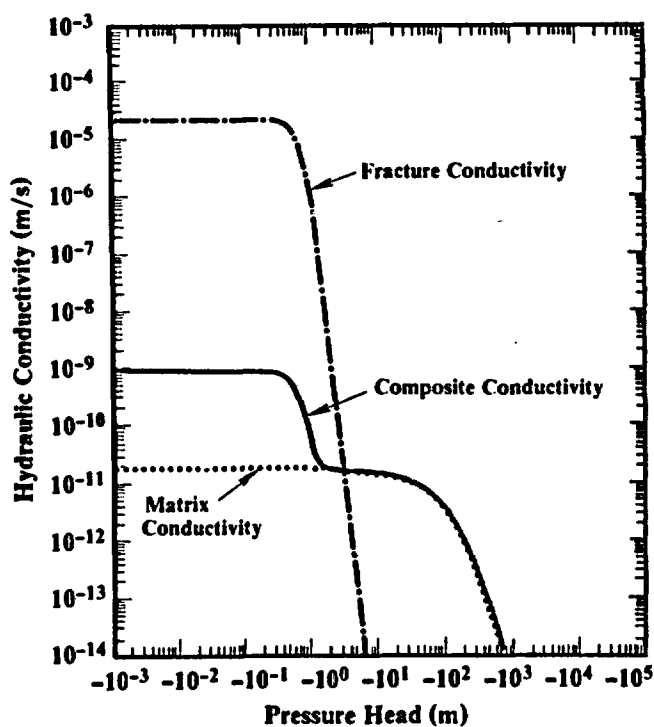


Figure A9. Hydraulic Conductivity Versus Pressure Head for Unit C

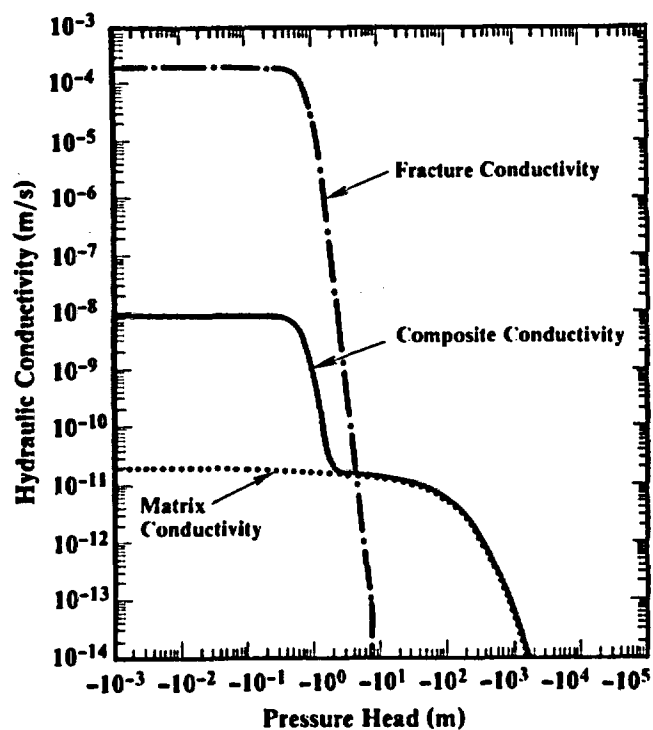


Figure A11. Hydraulic Conductivity Versus Pressure Head for Zeolitic Unit Ez

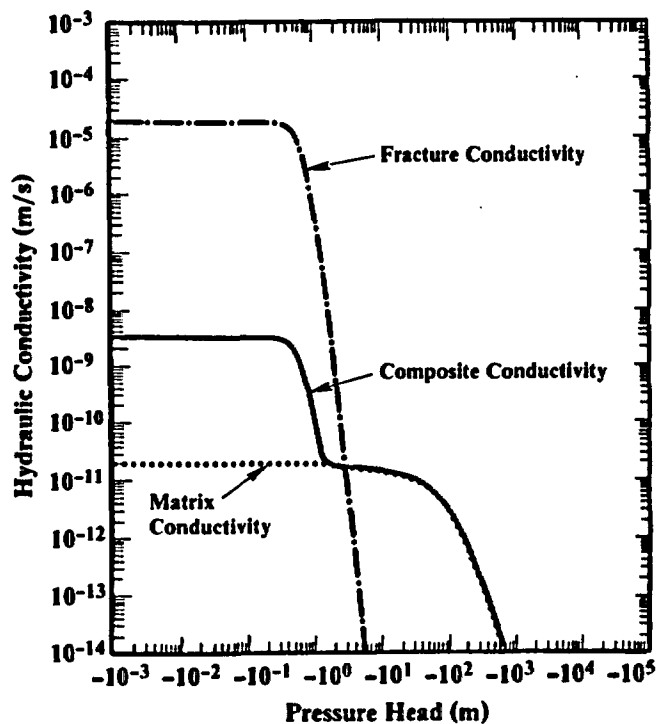


Figure A10. Hydraulic Conductivity Versus Pressure Head for Unit D

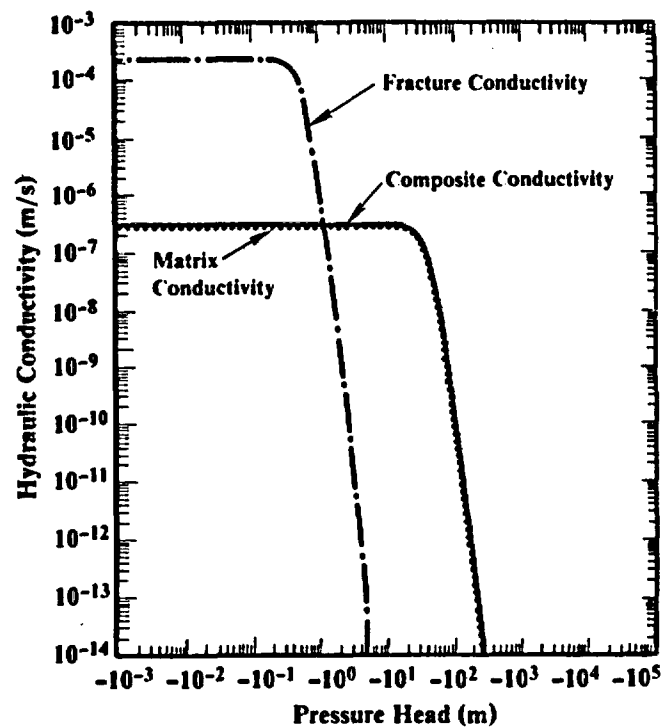


Figure A12. Hydraulic Conductivity Versus Pressure Head for Vitric Unit Ev

APPENDIX B

NNWSI Data Base Information

The analyses outlined in this paper are generic in nature and do not represent the proposed nuclear-waste-repository site at Yucca Mountain, Nevada. Therefore, requirements for conformance to the Nevada Nuclear Waste Storage Investigations (NNWSI) Project Reference Information Base do not apply. Also, no data are reported here that are appropriate for inclusion in the NNWSI Project Site and Engineering Properties Data Base.

DISTRIBUTION:

Lawrence Berkeley Laboratory (2)
Earth Sciences Division
Attn: M. Alavi
T. N. Narasimhan
1 Cyclotron Road
Berkeley, CA 94720

OAQ Corp.
Attn: W. Beyeler
PO Box 277
Tijeras, NM 87059

Pacific Northwest Laboratories (2)
Attn: C. Cole
J. Depner
PO Box 999
Richland, WA 99352

Lawrence Livermore National (2)
Laboratory
Attn: K. Eggert
J. Nitao
MS L-202
Livermore, CA 94550

Los Alamos National Laboratory (3)
Attn: K. Birdsell
E. Greenwade
B. Travis
MS-F665
Los Alamos, NM 87545

Holcomb Research Institute
Butler University
Attn: D. Mach
4600 Sunset Avenue
Indianapolis, IN 46208

US Department of Energy
Attn: J. Rotert
2753 South Highland Avenue
Las Vegas, NV 89114

US Geological Survey (5)
Denver Federal Center
Attn: D. Hoxie
P. Montazer
J. Reed
G. Ryals
W. Wilson
Box 25046, MS-416
Lakewood, CO 80225

US Nuclear Regulatory Commission (3)
Waste Management Branch
Division of Engineering Safety
Attn: T. McCartin
T. Nicholson
F. Costanzi
MS NL-007
Washington, DC 20555

Spectra Research Institute (3)
Attn: A. Dudley
J. H. Gauthier
N. Zieman
3700 Osuna NE, Suite 503
Albuquerque, NM 87109

Science Applications
International Corp.
The Valley Bank Center
Attn: M. Teubner
101 Convention Center Dr.
Suite 407
Las Vegas, NV 89109

Science Applications
International Corp.
Attn: D. Updegraff
2109 Air Park Road, SE
Albuquerque, NM 87106

Swedish Nuclear Power Inspectorate
Attn: K. Andersson
Box 27106
S-102 52 Stockholm
SWEDEN

Swedish Nuclear and Fuel Waste
Management Co. (SKB)
Attn: G. Baeckblom
Box 5864
S-102 48 Stockholm
SWEDEN

British Geological Survey
Macleon Building
Attn: J. Barker
Wallingford
Oxfordshire OX10 8BB
UNITED KINGDOM

DISTRIBUTION (continued):

Gesellschaft fur Reaktorsicherheit
Attn: P. Bogorinski
Schwertnergasse 1
D-5000 Koln 1
FEDERAL REPUBLIC OF GERMANY

Atkins Research and Development
Woodcote Grove
Attn: T. Broyd
Ashley Road
Epsom
Surrey KT18 5BW
UNITED KINGDOM

Gesellschaft fur Strahlen- und
Umweltforschung (GSF)
Technical University of Berlin
Attn: E. Butow
Marchstrasse 18
D-1000 Berlin 10
FEDERAL REPUBLIC OF GERMANY

Atomic Energy of Canada Ltd.
Attn: T. Chan
WNRE, Station 40
Pinawa
Manitoba ROE 1L0
CANADA

Rockwell Hanford Operations
Basalt Waste Isolation Project
Attn: P. Clifton
PO Box 800
Richland, WA 99352

US Nuclear Regulatory Commission
Geotechnical Branch
Office of Nuclear Material Safety
and Safeguards
Attn: R. Codell
Washington, DC 20555

MS RW-40
Department of Energy
Attn: C. Cooley
1000 Independence Avenue
Washington, DC 20585

Atomic Energy of Canada Ltd.
Whiteshell Nuclear Research
Establishment
Attn: K. Dormuth
Pinawa
Manitoba ROE 1L0
CANADA

MS RW-232
Department of Energy
Attn: N. Eisenberg
1000 Independence Avenue
Washington, DC 20585

National Institute of Public Health
and Environmental Hygiene (RIVM)
Attn: P. Glasbergen
PO Box 150
2260 ad Leidschendam
NETHERLANDS

Ecole des Mines
Attn: P. Goblet
35, Rue Saint-Honore
F-77305 Fontainebleau
FRANCE

KEMAKTA Consultants Co.
Attn: B. Grundfelt
Pipersgatan 27
S-112 28 Stockholm
SWEDEN

Office of Nuclear Waste Isolation
Battelle Project Management Division
Attn: S. Gupta
505 King Avenue
Columbus, OH 43201

Battelle Project Management Division
Office of Waste Technology Development
Attn: B. Gureghian
7000 S. Adams Street
Willowbrook, IL 60521

Eidg. Institut fur
Reaktorforschung (EIR)
Attn: J. Hadermann
CH-5303 Wurenlingen
SWITZERLAND

DISTRIBUTION (continued):

Theoretical Physics Division
Attn: A. Herbert
AERE
Harwell Oxfordshire
GBR-Didcot Oxon OX11 0RA
UNITED KINGDOM

Institut für Kerntechnik der
Technische Universität Berlin
Attn: L. Heredia
Marchstrasse 18
D-1000 Berlin 10
FEDERAL REPUBLIC OF GERMANY

Theoretical Physics Division
Attn: D. Hodgkinson
AERE
Harwell, Oxfordshire
GBR-Didcot Oxon OX11 0RA
UNITED KINGDOM

Gesellschaft für Strahlen- und
Umweltforschung (GSF)
Technical University of Berlin
Attn: E. Holzbecher
Marchstrasse 18
D-1000 Berlin 10
FEDERAL REPUBLIC OF GERMANY

Motor Columbus
Ingenieurunternehmung AG
Attn: W. Huerlimann
Parkstrasse 27
CH-5401 Baden
SWITZERLAND

Nationale Genossenschaft für die
Lagerung Radioaktiver Abfälle
(NAGRA)
Attn: P. Hufschmied
Parkstrasse 23
CH-5401 Baden
SWITZERLAND

Theoretical Physics Division
Attn: P. Jackson
AERE
Harwell, Oxfordshire
GBR-Didcot Oxon OX11 0RA
UNITED KINGDOM

Swedish Nuclear Power Inspectorate
Attn: F. Kautsky
Box 27106
S-102 52 Stockholm
SWEDEN

Nuclear Environment Section
Environment Department
Civil Engineering Department
Central Research Institute of Electric
Power Industry (CRIEPI)
Attn: M. Kawanishi
1-646, Abiko
Abiko City
Chiba-Prefecture
JAPAN

JAERI
Attn: H. Kimura
Tokai-Mura
Naka-gun
Ibaraki-ken
JAPAN 319-11

Universite de Neuchatel
Centre d'Hydrogeologie de l'Universite
Attn: L. Kiraly
Rue Emile-Argand 11
CH-2000 Neuchatel
SWITZERLAND

Civil Engineering Laboratory
Technical Research Institute
Hazama-Gumi Ltd.
Attn: H. Kojo
4-17-23
Honcho-nishi
Yono
Saitama
338
JAPAN

Swedish Nuclear Power Inspectorate
Attn: A. Larsson
Box 27106
S-102 52 Stockholm
SWEDEN

DISTRIBUTION (continued):

National Institute of Public Health
and Environmental Hygiene (RIVM)
Attn: T. Leijnse
PO Box 150
2260 ad Leidschendam
NETHERLANDS

KEMAKTA Consultants Co.
Attn: B. Lindbom
Pipersgatan 27
S-112 28 Stockholm
SWEDEN

Departement d'Analyse de Surete
Commissariat a l'Energie Atomique
Institut de Protection et de
Surete Nucleaire
Attn: J. Lewi
B.P. No. 6
F-99260 Fontenay-Aux-Roses
FRANCE

Okumura Corporation
Geotechnical Research Section
Tsukuba Research Institute
Attn: H. Masui
387 Suka, Ohsuna
Oho-cho
Tsukuba-gun
Ibaraki
300-33
JAPAN

Technical Research Centre of Finland
Nuclear Engineering Laboratory
Attn: K. Meling
Loennrotinkatu 37
PO Box 169
SF-001 81 Helsinki
FINLAND

National Insitute of Radiation
Protection
Attn: L. Moberg
Box 60204
S-104 01 Stockholm
SWEDEN

JAERI
Division of Environmental Safety
Research
Attn: S. Muraoka
Tokai-mura
Naka-gun
Ibaraki-ken
JAPAN 319-11

JAERI
Chief of HLW Management Research
Laboratory
Division of Environmentl Safety
Research
Attn: H. Nakamura
Tokai-mura
Naka-gun
Ibaraki-ken
JAPAN 319-11

British Geological Survey
Attn: D. Noy
Keyworth
Nottingham NG12 5GG
UNITED KINGDOM

School of Civil Engineering
Kyoto University
Attn: Y. Ohnishi
Kyoto 606
JAPAN

Atkins Research and Development
Woodcote Grove
Ashley Road
Attn: R. Paige
Epsom
Surrey KT18 5BW
UNITED KINGDOM

Teollisuuden Voima Oy (TVO)
Attn: E. Peltonen
Fredrikinkatu 51-53
SF-00100 Helsinki 10
FINLAND

CEA/IPSN
DAS/SAED, CEN.FAR.
Attn: P. Raimbault
B.P. No. 6
F-92260 Fontenay-Aux-Roses
FRANCE

DISTRIBUTION (continued):

Motor Columbus
Ingenieurunternehmung AG
Attn: G. Resele
Parkstrasse 27
CH-5401 Baden
SWITZERLAND

Rockwell Hanford Operations
Basalt Waste Isolation Project
Attn: B. Sagar
PO Box 800
Richland, WA 99352

Teollisuuden Voima OY (TVO)
Attn: J-P Salo
Fredrikinkatu 51-53
SF-001 00 Helsinki 10
FINLAND

National Institute of Public Health
and Environmental Hygiene (RIVM)
Attn: F. Sauter
PO Box 150
2260 ad Leidschendam
NETHERLANDS

Atomic Energy of Canada Ltd
Attn: N. W. Scheir
WNRE, Station 40
Pinawa
Manitoba ROE 1L0
CANADA

Bundesanstalt fur Geowissenschaften
und Rohstoffe
Attn: K. Schelkes
Stilleweg 2
3000 Hannover 51
FEDERAL REPUBLIC OF GERMANY

OECD
Nuclear Energy Agency
Attn: C. Thegerstroem
38, Boulevard Suchet
F-75016 Paris
FRANCE

Royal Institute of Technology
Attn: R. Thunvik
S-100 44 Stockholm
SWEDEN

Laboratory of Hydraulics, Hydrology
and Glaciology
Attn: J. Troesch
ETH-Zurich
8092 Zurich
SWITZERLAND

Institute for Energy Technology
Attn: U. Tveten
Boks 40
N-2007 Kjeller
NORWAY

US Geological Survey
Water Resources Division
Attn: C. Voss
431 National Center
Reston, VA 22092

Technical Research Centre of Finland
Nuclear Engineering Laboratory
Attn: S. Vuori
Loennrotinkatu 37
PO Box 169
SF-001 81 Helsinki
FINLAND

Motor Columbus Ingenieurunternehmung AG
Attn: C. Wacker
Parkstrasse 27
CH-5401 Baden
SWITZERLAND

Technical Research Centre of Finland
Nuclear Engineering Laboratory
Attn: M. Winberg
Loennrotinkatu 37
PO Box 169
SF-001 81 Helsinki
FINLAND

Director
Office of Civilian Radioactive
Waste Management
US Department of Energy
Attn: B. C. Rusche (RW-1)
Forrestal Building
Washington, DC 20585

DISTRIBUTION (continued):

Office of Civilian Radioactive
Waste Management
US Department of Energy
Attn: R. Stein (RW-23)
Forrestal Building
Washington, DC 20585

Office of Civilian Radioactive
Waste Management
US Department of Energy
Attn: J. J. Fiore, (RW-221)
Forrestal Building
Washington, DC 20585

Office of Civilian Radioactive
Waste Management
US Department of Energy
Attn: M. W. Frei (RW-231)
Forrestal Building
Washington, DC 20585

Siting Division
Office of Geologic Repositories
US Department of Energy
Attn: E. S. Burton (RW-25)
Forrestal Building
Washington, DC 20585

Geosciences & Technology Division
Office of Geologic Repositories
US Department of Energy
Attn: C. R. Cooley (RW-24)
Forrestal Building
Washington, DC 20585

Office of Civilian Radioactive
Waste Management
US Department of Energy
Attn: V. J. Cassella (RW-222)
Forrestal Building
Washington, DC 20585

Program Management Division
Office of Geologic Repositories
US Department of Energy
Attn: T. P. Longo (RW-25)
Forrestal Building
Washington, DC 20585

Geosciences & Technology Division
Office of Geologic Repositories
US Department of Energy
Attn: C. Klingsberg (RW-24)
Forrestal Building
Washington, DC 20585

Office of Civilian Radioactive
Waste Management
US Department of Energy
Attn: B. G. Gale (RW-223)
Forrestal Building
Washington, DC 20585

Program Management Division
Office of Geologic Repositories
US Department of Energy
Attn: R. J. Blaney (RW-22)
Forrestal Building
Washington, DC 20585

Office of Civilian Radioactive
Waste Management
US Department of Energy
Attn: R. W. Gale (RW-40)
Forrestal Building
Washington, DC 20585

Outreach Programs
Office of Policy, Integration and
Outreach
US Department of Energy
Attn: J. E. Shaheen (RW-44)
Forrestal Building
Washington, DC 20585

Salt Repository Project Office
US Department of Energy
Attn: J. O. Neff, Manager
505 King Avenue
Columbus, OH 43201

Engineering & Licensing Division
Office of Geologic Repositories
US Department of Energy
Attn: D. C. Newton (RW-23)
Forrestal Building
Washington, DC 20585

DISTRIBUTION (continued):

Basalt Waste Isolation Project Office
Richland Operations Office
US Department of Energy
Attn: O. L. Olson, Manager
PO Box 550
Richland, WA 99352

Waste Management Project Office (4)
US Department of Energy
Attn: D. L. Vieth, Director
PO Box 14100
Las Vegas, NV 89114

Office of Public Affairs
US Department of Energy
Attn: D. F. Miller, Director
PO Box 14100
US Department of Energy
Las Vegas, NV 89114

Office of Public Affairs (12)
US Department of Energy
Attn: P. M. Bodin
PO Box 14100
Las Vegas, NV 89114

Health Physics Division
US Department of Energy
Attn: B. W. Church, Director
PO Box 14100
Las Vegas, NV 89114

Chief, Repository Projects Branch
Division of Waste Management
US Nuclear Regulatory Commission
Washington, DC 20555

Document Control Center
Division of Waste Management
US Nuclear Regulatory Commission
Washington, DC 20555

Crystalline Rock Project Office
US Department of Energy
Attn: S. A. Mann, Manager
9800 South Cass Avenue
Argonne, IL 60439

Lawrence Livermore National
Laboratory
Attn: K. Street, Jr.
PO Box 808
Mail Stop L-209
Livermore, CA 94550

Technical Project Officer for NNWSI (3)
Lawrence Livermore National
Laboratory
Attn: L. D. Ramspott
PO Box 808
Mail Stop L-204
Livermore, CA 94550

Associate Director
Office of Civilian Radioactive
Waste Management
US Department of Energy
Attn: W. J. Purcell (RW-20)
Forrestal Building
Washington, DC 20585

Technical Project Officer for NNWSI (4)
Los Alamos National Laboratory
Attn: D. T. Oakley
PO Box 1663
Mail Stop F-619
Los Alamos, NM 87545

Technical Project Officer for NNWSI (3)
US Geological Survey
Attn: L. R. Hayes
PO Box 25046
421 Federal Center
Denver, CO 80225

NTS Section Leader
Repository Project Branch
Division of Waste Management
US Nuclear Regulatory Commission
Washington, DC 20555

US Geological Survey
Attn: V. M. Glanzman
PO Box 25046
913 Federal Center
Denver, CO 80225

DISTRIBUTION (continued):

NRC Site Representative
Attn: P. T. Prestholt
1050 East Flamingo Road
Suite 319
Las Vegas, NV 89109

Technical Project Officer for NNWSI
Science Applications
International Corporation
Attn: M. E. Spaeth
Suite 407
101 Convention Center Drive
Las Vegas, NV 89109

SAIC-T&MSS Library (2)
Science Applications
International Corporation
Suite 407
101 Convention Center Drive
Las Vegas, NV 89109

Science Applications
International Corp.
Attn: W. S. Twenhofel, Consultant
820 Estes Street
Lakewood, CO 89215

Energy Support Division
Holmes & Narver, Inc.
Attn: A. E. Gurrola, General Manager
Mail Stop 580
PO Box 14340
Las Vegas, NV 89114

Las Vegas Branch
Fenix & Scisson, Inc.
Attn: J. A. Cross, Manager
Mail Stop 514
PO Box 14308
Las Vegas, NV 89114

Office of Policy, Integration, and
Outreach
US Department of Energy
Attn: N. Duncan (RW-44)
Forrestal Building
Washington, DC 20585

Technical Project Officer for NNWSI
Westinghouse Electric Corporation
Waste Technology Services Division
Nevada Operations
Attn: J. S. Wright
PO Box 708
Mail Stop 703
Mercury, NV 89023

ONWI Library
Battelle Columbus Laboratory
Office of Nuclear Waste Isolation
505 King Avenue
Columbus, OH 43201

Roy F. Weston, Inc.
Attn: W. M. Hewitt, Program Manager
955 L'Enfant Plaza, Southwest, Suite 800
Washington, DC 20024

General Manager
Reynolds Electrical &
Engineering Co., Inc.
Attn: H. D. Cunningham
PO Box 14400
Mail Stop 555
Las Vegas, NV 89114

Office of the Governor
Attn: T. Hay, Executive Assistant
State of Nevada
Capitol Complex
Carson City, NV 89710

Nuclear Waste Project Office (3)
Attn: R. R. Loux, Jr., Executive Director
State of Nevada
Evergreen Center, Suite 252
1802 North Carson Street
Carson City, NV 89701

Program Manager
Nuclear Waste Project Office
Attn: C. H. Johnson, Technical
State of Nevada
Evergreen Center, Suite 252
1802 North Carson Street
Carson City, NV 89701

DISTRIBUTION (continued):

Desert Research Institute
Water Resources Center
Attn: J. Fordham
PO Box 60220
Reno, NV 89506

Department of Comprehensive
Planning
Clark County
225 Bridger Avenue, 7th Floor
Las Vegas, NV 89155

Lincoln County Commission
Lincoln County
PO Box 90
Pioche, NV 89043

Community Planning and
Development
City of North Las Vegas
PO Box 4086
North Las Vegas, NV 89030

City Manager
City of Henderson
Henderson, NV 89015

Project Manager
Bechtel National Inc.
Attn: N. A. Norman
PO Box 3965
San Francisco, CA 94119

Los Alamos Technical Associates
Attn: F. Butler
1650 Trinity Drive
Los Alamos, New Mexico 87544

Science Applications
International Corporation
Attn: T. G. Barbour
1626 Cole Boulevard, Suite 270
Golden, CO 80401

Field Systems Group Leader
Attn: E. P. Binnall
Building 50B/4235
Lawrence Berkeley Laboratory
Berkeley, CA 94720

Desert Research Institute
Attn: M. Mifflin
Water Resources Center
Suite 1
2505 Chandler Avenue
Las Vegas, NV 89120

Planning Department
Nye County
PO Box 153
Tonopah, NV 89049

Economic Development
Department
City of Las Vegas
400 East Stewart Avenue
Las Vegas, NV 89101

Director of Community
Planning
City of Boulder City
PO Box 367
Boulder City, NV 89005

Commission of the
European Communities
200 Rue de la Loi
B-1049 Brussels
BELGIUM

Technical Information Center
Roy F. Weston, Inc.
955 L'Enfant Plaza, Southwest
Suite 800
Washington, DC 20024

Parsons Brinkerhoff Quade &
Douglas, Inc.
Attn: R. Harig
1625 Van Ness Ave.
San Francisco, CA 94109-3678

Engineers International, Inc.
Attn: M. M. Singh, President
98 East Naperville Road
Westmont, IL 60559-1595

Itasca Consulting Group, Inc.
Attn: R. Hart
PO Box 14806
Minneapolis, Minnesota 55414

DISTRIBUTION (continued):

Office of Civilian Radioactive
Waste Management
US Department of Energy
Attn: T. H. Isaacs (RW-22)
Forrestal Building
Washington, DC 20585

Office of Civilian Radioactive
Waste Management
US Department of Energy
Attn: D. H. Alexander (RW-232)
Forrestal Building
Washington, DC 20585

Basalt Waste Isolation Project (2)
Library
Rockwell Hanford Operations
Attn: B. J. King, Librarian
PO Box 800
Richland, WA 99352

RE/SPEC Inc.
Attn: D. K. Parrish
3815 Eubank, NE
Albuquerque, NM 87191

Reynolds Electrical & Engineering
Co., Inc.
Attn: D. L. Fraser, General Manager
Mail Stop 555
PO Box 14400
Las Vegas, NV 89114-4400

Office of Civilian Radioactive
Waste Management
US Department of Energy
Attn: G. Parker (RW-241)
Forrestal Building
Washington, DC 20585

Office of Civilian Radioactive
Waste Management
US Department of Energy
Attn: J. P. Knight (RW-24)
Forrestal Building
Washington, DC 20585

Office of Civilian Radioactive
Waste Management
US Department of Energy
Attn: A. Jelacic (RW-233)
Forrestal Building
Washington, DC 20585

Deputy Assistant Director
for Engineering Geology
US Geological Survey
Attn: J. R. Rollo
106 National Center
12201 Sunrise Valley Drive
Reston, VA 22092

United States Bureau of Mines
Attn: R. Lindsay Mundell
PO Box 25086
Building 20
Denver Federal Center
Denver, Colorado 80225

Technical Project Officer for NNWSI
Reynolds Electrical & Engineering
Co., Inc.
Attn: V. Gong
Mail Stop 615
PO Box 14400
Las Vegas, NV 89114-4400

J. F. T. Agapito Associates, Inc.
Attn: C. M. St. John
27520 Hawthorne Blvd., Suite 137
Rolling Hills Estates, CA 90274

Technical Project Officer for NNWSI
Holmes & Narver, Inc.
Attn: J. P. Pedalino
Mail Stop 605
PO Box 14340
Las Vegas, NV 89114

Mountain West Research-Southwest, Inc.
Attn: E. Anderson
398 South Mill Avenue, Suite 300
Tempe, AZ 85281

City of Caliente (5)
Attn: J. Foremaster
PO Box 158
Caliente, NV 89008

Technical Project Officer for NNWSI
Fenix & Scisson, Inc.
Attn: S. D. Murphy
Mail Stop 514
PO Box 15408
Las Vegas, NV 89114

DISTRIBUTION (continued):

Office of Civilian Radioactive
Waste Management
US Department of Energy
Attn: S. H. Kale (RW-20)
Forrestal Building
Washington, DC 20585

Manager for Commercial
Nuclear Waste
Basalt Waste Isolation Project
Office
US Department of Energy
Attn: J. H. Anttonen, Deputy Assistant
PO Box 550
Richland, WA 99352

1511 D. K. Gartling
1511 N. E. Bixler
1511 R. R. Eaton
1511 P. L. Hopkins
6300 R. W. Lynch
6310 T. O. Hunter
6310 72/12144/17/Q3
6310 NNWSICF
6311 A. L. Stevens
6311 C. Mora
6312 F. W. Bingham
6312 G. E. Barr
6312 M. L. Green
6312 B. S. Langkopf

6312 R. R. Peters
6312 A. C. Peterson
6312 R. W. Prindle (10)
6312 M. S. Tierney
6312 J. G. Yeager
6313 T. E. Blejwas
6313 E. A. Klavetter
6314 J. R. Tillerson
6314 J. A. Fernandez
6315 S. Sinnock
6315 P. C. Kaplan
6316 R. B. Pope
6330 W. D. Weart
6332 L. D. Tyler
6332 R. Beraun
6332 WMT Library (20)
6410 N. R. Ortiz
6416 R. M. Cranwell
6416 E. J. Bonano
6416 P. A. Davis
6416 R. P. Rechard
7223 R. G. Easterling
7223 B. M. Rutherford
7223 F. W. Spencer
8024 P. W. Dean
3141 S. A. Landenberger (5)
3151 W. L. Garner (3)
3154-3 C. H. Dalin (28)
For DOE/OSTI (Unlimited Release)

